2019-01-01

Interference Mitigation of Adjacent Radio Frequency Signals on a Flexible Software-Defined Radio Testbed Platform

Mirza Mohammad Maqbule Maqbule Elahi
University of Texas at El Paso, mmmelahi91@gmail.com

INTERFERENCE MITIGATION OF ADJACENT RADIO FREQUENCY SIGNALS ON A FLEXIBLE SOFTWARE-DEFINED RADIO TESTBED PLATFORM

MIRZA MOHAMMAD MAQBULE ELAHI

Master's Program in Computational Science

APPROVED:

Virgilio Gonzalez, Ph.D., Chair

Benjamin Flores, Ph.D.

Rosa Fitzgerald, Ph.D.

Stephen Crites, Ph.D.
Dean of the Graduate School

Dedication

I would like to dedicate my thesis paper to my loving parents Mr. and Mrs. Elahi, and my siblings for their constant motivation in pursuing my graduate studies.

INTERFERENCE MITIGATION OF ADJACENT RADIO FREQUENCY SIGNALS ON A FLEXIBLE SOFTWARE-DEFINED RADIO TESTBED PLATFORM

by

MIRZA MOHAMMAD MAQBULE ELAHI, B.Sc.

THESIS

Presented to the Faculty of the Graduate School of

The University of Texas at El Paso

in Partial Fulfillment

of the Requirements

for the Degree of

MASTER OF SCIENCE

Computational Science Program

THE UNIVERSITY OF TEXAS AT EL PASO

May 2019

Acknowledgements

I would like to express my gratitude to Dr. Virgilio Gonzalez, Associate Chair of the Electrical and Computer Engineering (ECE) Department at the University of Texas at El Paso (UTEP) for his constant support and guidance towards my progress in graduate studies. Dr. Gonzalez is an amazing tutor in class and a wonderful person as a research advisor with plenty of technical knowledge. As a faculty member of the ECE Department he inspires me to pursue teaching as a profession.

I would like to thank my co-workers Juan Gonzalez and Jose Castillo for their dedication and help with our research project. I have to mention Mr. Pabel Corral and Mr. Susumu "Duke" Yasuda from White Sands Missile Range for their full co-operation with the ongoing Spectrum Management Project. It has been my pleasure to work with these amazing people, or I would like to call them a friend. I look forward to crossing path with them in the future.

My appreciation goes to the Computational Science (CPS) Program and ECE Department for their support. Also, my friends from the Bangladesh Student Association have been a great inspiration.

Abstract

The radio frequency (RF) spectrum is crowded with users and adjacent frequency users are facing an increase in interference from each other. The spectrum governing body Federal Communications Commission (FCC) has the difficult task of allocating spectral bands for new users for mobile devices using 4G LTE technology. Telemetry is affected by the adjacent band 4G LTE users in terms of signal degradation. To minimize the interference between adjacent frequency users, several methods can be used. A common but inefficient method separates adjacent band frequencies using guard bands which leaves a big portion of the spectrum unused. Alternatively, adjacent RF signals can be separated using digital filtering techniques with the signal of interest being unharmed and reducing the signal power of the interfering signal. A digital filtering technique includes bandpass filter (BPF) rejection, which has the ability to filter out adjacent interfering signals. This is accomplished by designing bandpass digital filters where the passband and stopband frequencies are adjusted to achieve maximum signal power and reject the interfering signal by reducing its power. A flexible software-defined radio testbed is set up to experiment and analyze this scenario with ease and effective measures.

Keywords: Radio frequency, Telemetry, 4G LTE, adjacent signal, interference, digital filter, bandpass.

Table of Contents

List of Tables

List of Figures

List of Illustrations

Chapter 1: Introduction

The spectral bands reserved for military use is being readjusted to fit the consumer need for mobile data and applications. The government agencies like NTIA and FCC have sought measures to avoid harmful interference from the spectrum users. Aeronautical Mobile Telemetry (AMT) is affected in the presence of adjacent band 4G Long-Term Evolution (LTE) spectrum users. The primary user of the AMT bands includes White Sands Missile Range (WSMR). For uninterrupted services spectrum management techniques are adopted. A possible solution is to identify and classify the readjustments in the spectrum band by creating a flexible testbed which can emulate the said systems.

This thesis paper describes a series of controlled laboratory measurements of key parameters on a simulated Software-defined Radio (SDR) testbed which includes methodology, test execution, and the data analysis of interference mitigation. Laboratory tests were done to mix signals in the adjacent band and analyze their performance.

There is an exponential increase in number of devices, users and traffic, service providers are facing a challenge of spectrum drought. The Commerce Spectrum Management Advisory Committee (CSMAC) has some recommendations to reduce interference from adjacent bands and thus facilitating efficient use of spectrum. Although the use of guardbands is a very common and historic practice but it is not the preferred mechanism nowadays to prevent interference. The development of dynamic spectrum access (DSA) techniques provides a more flexible and efficient use of the spectrum. This includes the database approaches and spectrum sensing technologies.

Cognitive radio (CR) and spectrum sensing technologies are considered to be an important tool for spectrum sharing and interference mitigation. Spectrum sensing devices are capable of

protecting services that uses different modulation systems. Rigorous testing and evaluation can help ensure an adaptive system with the capabilities of CR and spectrum sensing which can reduce interference.

Filtering solutions are also considered to eliminate interference from adjacent radio frequency signals. For simplicity, narrowband Amplitude Modulated (AM) signals are generated in adjacent bands and the power level of the signals are observed in presence of a bandpass rejection filter. The bandpass filter with adjustable parameters like passband and stopband frequencies provides flexibility. An Analog filter equipped in a 2.4m Tracker was acquired by WSMR to mitigate the interference from 4G LTE bands. The proposed rejection level of the filter was 60 to 70 dB. Digital filtering technique is a very effective application in mitigating interference between adjacent spectrum users. It rejects the adjacent interfering signal by reducing its signal power. This can be achieved in the laboratory by designing filters with the desired rejection levels on a flexible testbed.

SDRs can be used to identify and classify spectrum users based on their modulation type, signal power, Signal-to-Noise Ratio (SNR), bandwidth and the technology: Wi-Fi, 4G-LTE etc. The results will be stored into a database for the purpose of finding solutions for interference mitigation with the techniques mentioned earlier.

Chapter 2: Literature Review

2.1 Problem History

The radio frequency standards for Aeronautical Mobile Telemetry (AMT) are defined in the Manual of Regulations and Procedures for Federal Radio Frequency Management [1]. The purpose of the standards is to determine the equipment and frequency allocation for an interference free utilization of the radio frequency (RF) spectrum. For smooth test operations between ranges these standards deliver a general framework for data transfer and support.

The reallocation of the Telemetry bands caused a reduced spectrum available for the military use. The bands for commercial use, like spectrum in 1695 – 1710 MHz, 1755 – 1780 MHz, and 2155 – 2180 MHz, previously allocated for military use. These are also known as AWS-3 bands which were allocated during Auction 97 [2]. A total of 65 MHz of spectrum were dedicated ensuring high speed and greater capacity required for the growing demand of the wireless services.

The loss of spectrum resulted in increased interference for the Telemetry users from the adjacent spectrum users. The interference levels can be measured using state of the art radio devices which can be configured to replicate the real time signal. In order to mitigate the interference, certain methods can be adopted which includes setting guard bands and digital filtering techniques [3].

2.2 Technology Foundation

The traditional radio devices have a simplified Communication System [4], which includes a message source, processing unit, transmitter, medium of transmission, a receiver, another processing unit, finally message destination as shown in Figure 1. The message processing is the

process of taking the source information and putting it into a format that can be transmitted over whichever medium is required. In a wireless or RF system, typical communication happens through free space or air, as opposed to through a cable/wire or a fiber network.

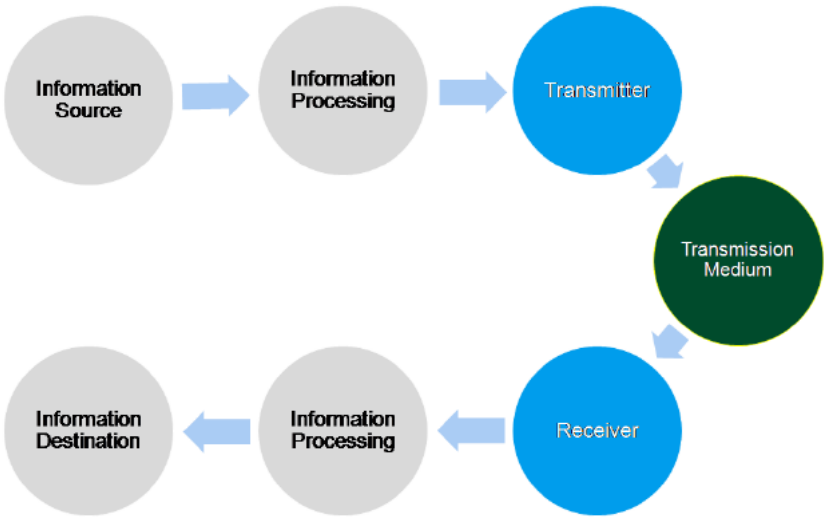

Figure 1: RF system with the transition of information from source to destination.

In early applications, it was more common to have a one-way path for the RF signals in RF design. Radio and television are good examples of the one-way path as large antennas transmitted signals one way to the radios and televisions. Today data is the major part of the communicated information where there is a two-way path for the RF signals. Mobile smart phones are a great example of a device, which can both transmit and receive data.

In the early days of wireless communications, most signals were sine waves. A sine wave can be represented with a frequency, an amplitude, and a phase.

$$V = Asin(\omega t + \varphi)$$

where A is the amplitude of the sine wave, $\omega = 2\pi f$ is the angular frequency, f is frequency and φ is the initial phase of the signal.

Figure 2 demonstrates two signals represented in the time domain. In terms of our communications system, the goal is to send message or information from a source to a destination by manipulating these sine waves. It is more often to have more complex digital signals nowadays.

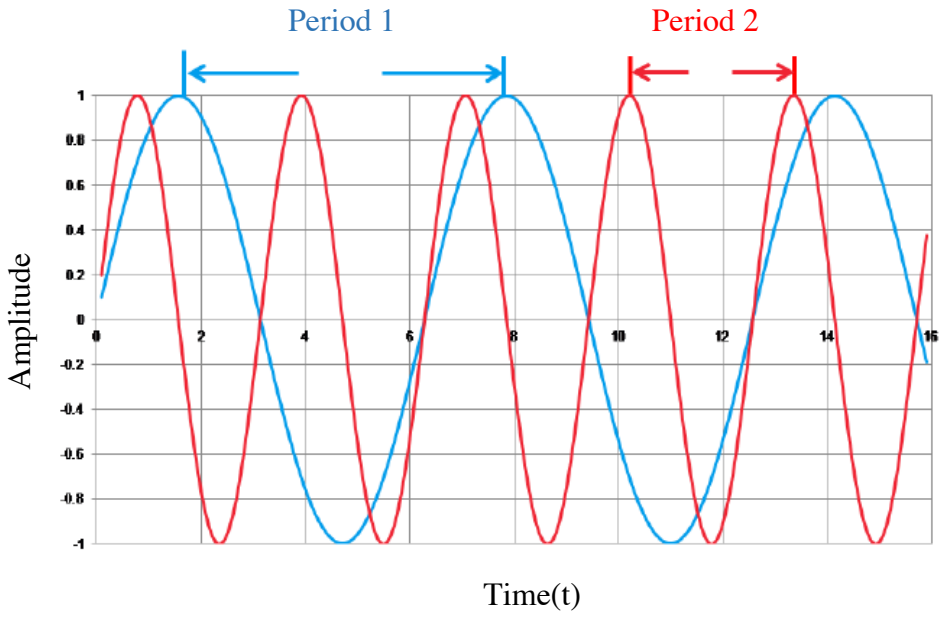

Figure 2: Sinusoidal waveforms with different time periods, sin(t) and sin(2t).

Typically, RF frequency domain is much preferred than the time domain. Figure 3 shows a spectrum sweep on a spectrum analyzer display. With the transmitted signals becoming more complex, modulated signals or signals with more information put on them, spectrum analyzer displays are better for understanding the multiple frequencies and modulation techniques. The output of the spectrum analyzer gives the peak of the signal in dB, bandwidth of the signal occupied in the spectral band and the spacing between the signals.

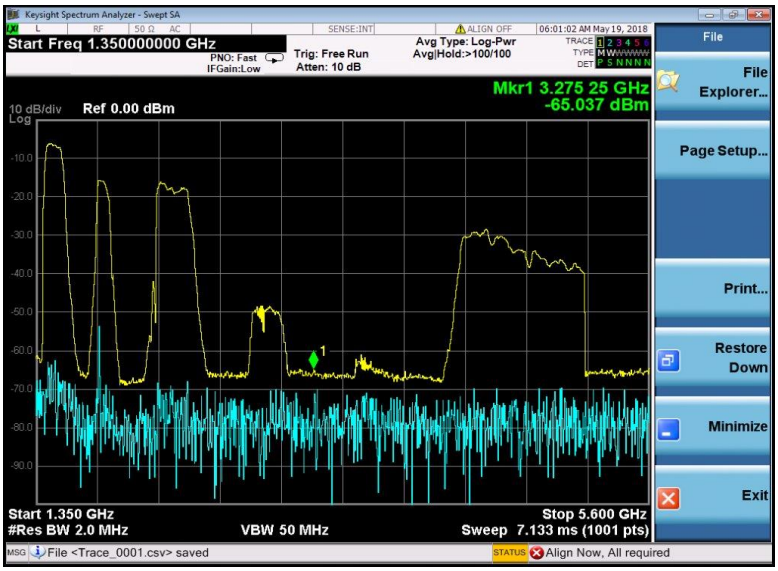

Figure 3: Spectrum sweep from 1.35 GHz to 5.60 GHz in RF band.

2.3 RELATED WORK

The large-scale simulation of interference from thousands of cellular base stations and their associated handsets will be a major activity for both the civil and DoD AMT communities as government spectrum is auctioned for use by commercial broadband carriers. There are documents which provide step-by-step procedure for accomplishing this. It can be implemented in a variety of ways, including as a collection of Excel spreadsheets in conjunction with the commercial software packages.

The Commerce Spectrum Management Advisory Committee (CSMAC) Working Group structure was created to explore ways to lower the repurposing costs and/or improve or facilitate commercial wireless industry access while protecting federal operations from adverse impact. Working Group 5 (WG-5) was specifically tasked with studying issues related to airborne operations in the 1755-1850 MHz band. Within WG-5, Sub-Working Group (SWG) Aeronautical Mobile Telemetry (AMT) was created to focus on issues related to Department of Defense (DOD) use of flight test telemetry operating in the band. Pursuant to the working group structure provided by the National Telecommunications and Information Administration (NTIA) the expected focus of work for WG-5 would be the 1) determination of protection requirements for federal operations,

and 2) understanding of the impact to commercial wireless of federal government airborne operations [5].

The level of interference from adjacent channels in AWS-3 bands have already been laid out in *Kip Temple's Paper* [6]. AMT spectrum users are constantly seeing new neighbors showing up in the form of cellular carriers in the adjacent channels. In the past AWS-3 AMT users have been worried primarily about in-band interferers, addressed within IRIG-106 Appendix A [7] as recommendations for channel spacing of AMT waveforms. Using assumptions about each link and choosing an interference geometry, the calculations revealed a distance a UE had to be from an AMT ground station to understand what given C/I means. This distance could be viewed as a "UE Keep Out Zone" around the AMT ground station. More analysis and interference scenarios need to be investigated particularly for scenarios requiring improved BER performance.

The process of spectrum allocation and how the results are going to be obtained through a testbed is explained in this Journal [8].The impacts of 4G LTE signal on TM signal was analyzed and the results of how the TM system affected the LTE system, their rules of interaction in order to keep the LTE system at an acceptable performance, and a brief introduction into how these results will aid in the 5G technologies by implementing a similar testbed were explained in this ITC 2018 Paper [9]. For the interference mitigation of the LTE system on the TM system, different rules must be followed to protect the TM system. In the LTE system, interference from the TM system was felt instantaneously and the performance of the link suffered greatly, the spectrum graph of the LTE Rx displayed both TM and LTE signals simultaneously, and its effects were seen clearly. For the TM system, the LTE signal remains masked as noise to the TM Rx, meaning that any LTE signal that gets closer and closer to the TM signal, will only be raising the noise level of the TM Rx, affecting its performance by increasing the FSER, reducing the channel capacity, and

affecting the visual parameters such as the constellation and eye diagrams. Interference mitigation using digital filtering techniques were also explored and published as a poster presentation [10].

Representatives from Edwards Air Force Base (EAFB) submitted a proposal to The National Advanced Spectrum and Communications Test Network (NASCTN) to measure long-term evolution (LTE) User Equipment (UE) emissions in the United States Advanced Wireless Service (AWS)-3 frequency band and aeronautical mobile telemetry (AMT) systems in the adjacent L band [11]. This proposal builds on and extends a previous NASCTN project that measured the out of band (OoB) LTE evolved Node B (eNB) and UE AWS-3 emissions into adjacent L and S (2200-2395 MHz) frequency band AMT systems. The results of the previous NASCTN project are documented in NIST Technical Note TN-1980 [1]. While the previous test measured general LTE OoB emissions, this project specifically measures the impact of interference on the AMT systems.

Cognitive Radio (CR) is a boosting factor for the efficient use of the radio spectrum [12]. Its adaptiveness and intelligence makes a traditional radio flexible and smart. A cognitive radio testbed can be used to verify concepts, algorithms and wireless protocols. A full-fledged cognitive radio is not yet demonstrated, but the development is ongoing on the key factors. Spectrum sensing [13] and spectrum allocation [14] are vital parts of CR. A SDR platform is suitable to build a cognitive radio testbed [15].

Chapter 3: Background

3.1 Spectrum Management & Radio Spectrum Allocation

The Federal and nonfederal agencies use of the radio frequency spectrum of 3 Hz to 300 GHz [16] for various operations whose distribution is governed by NTIA and FCC respectively. The 3G and 4G mobile services has created increased demand of the radio spectrum, which is limited in resource. These regulatory boards make the efficient use of spectrum by providing licenses to the government and nongovernment entities. Spectrum Auction is arranged to distribute licenses for mobile and wireless applications. Radio spectrum users can only transmit in the allocated frequency to avoid any violations to the FCC regulations.

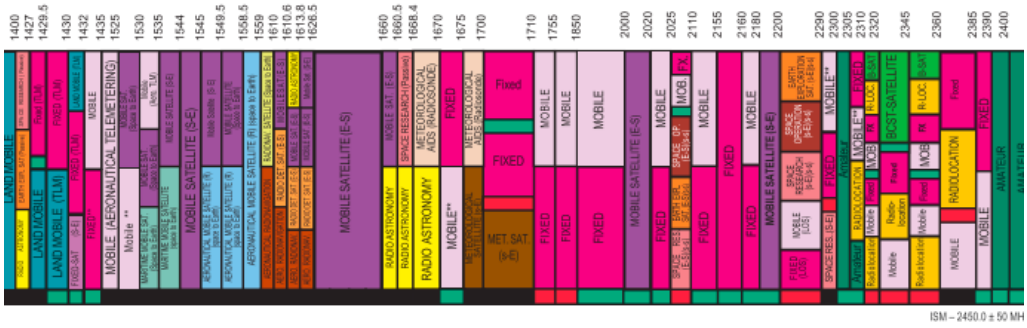

Figure 4: United States Radio Spectrum Allocation[1].

[1] https://www.ntia.doc.gov/files/ntia/publications/2003-allochrt.pdf

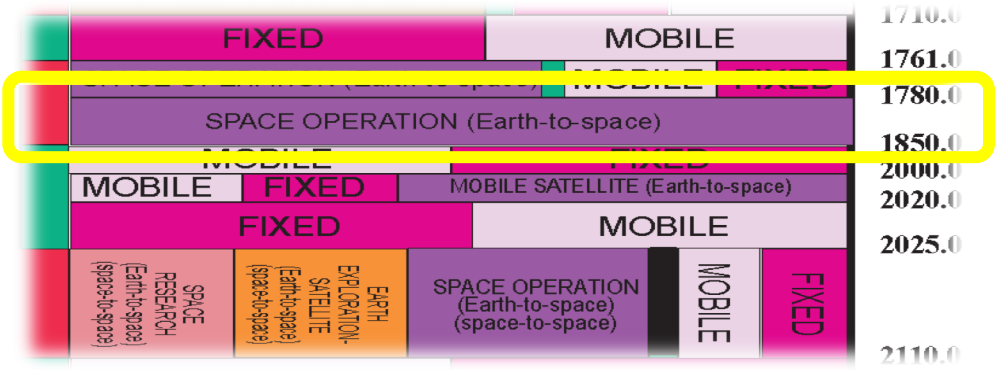

Figure 5: A closer look at the Telemetry band 1780 – 1850 MHz.

Different parts of the radio spectrum are allocated by the ITU for different radio transmission technologies and applications; some 40 radiocommunication services are defined in the ITU's Radio Regulations (RR).[2] In some cases, parts of the radio spectrum are sold or licensed to operators of private radio transmission services (for example, cellular telephone operators or broadcast television stations). Ranges of allocated frequencies are often referred to by their provisioned use (for example, cellular spectrum or television spectrum).[3] Because it is a fixed resource which is in demand by an increasing number of users, the radio spectrum has become increasingly congested in recent decades, and the need to utilize it more effectively is driving modern telecommunications innovations such as trunked radio systems, spread spectrum (ultra-wideband) transmission, frequency reuse, dynamic spectrum management, frequency pooling, and cognitive radio.

Ultra-high frequency UHF 300–3,000 MHz Television broadcasts, microwave oven, microwave devices/communications, radio astronomy, mobile phones, wireless LAN, Bluetooth, ZigBee, GPS and two-way radios such as land mobile, FRS and GMRS radios, amateur radio, satellite radio, Remote control Systems, ADSB. A radio band is a small contiguous section of the radio spectrum frequencies, in which channels are usually used or set aside for the same purpose.

To prevent interference and allow for efficient use of the radio spectrum, similar services are allocated in bands. For example, broadcasting, mobile radio, or navigation devices, will be allocated in non-overlapping ranges of frequencies.

Each of these bands has a basic band plan which dictates how it is to be used and shared, to avoid interference and to set protocol for the compatibility of transmitters and receivers.

3.2 SOFTWARE-DEFINED RADIO

Software-defined radio is a rapidly developing field that is driving the development of and innovation in communications technology and promises to significantly impact all communications sectors. With the exponential growth in the ways and means by which people need to communicate - data communications, voice communications, video communications, broadcast messaging, command and control communications, emergency response communications, etc. – modifying radio devices easily and cost-effectively has become business critical. Software-Defined Radio (SDR) [17] technology brings the flexibility, cost efficiency and power to drive communications forward, with wide-reaching benefits realized by service providers and product developers through to end users.

Several definitions can be found to describe Software Defined Radio, also known as Software Radio or SDR. The SDR Forum, working in collaboration with the Institute of Electrical and Electronic Engineers (IEEE) P1900.1 group, has worked to establish a definition of SDR that provides consistency and a clear overview of the technology and its associated benefits. Simply put Software Defined Radio is defined as:

"Radio in which some or all of the physical layer functions are software defined"

A radio is any kind of device that wirelessly transmits or receives signals in the radio frequency (RF) part of the electromagnetic spectrum to facilitate the transfer of information. In today's world, radios exist in a multitude of items such as cell phones, computers, car door openers, vehicles, and televisions.

Traditional hardware-based radio devices limit cross-functionality and can only be modified through physical intervention. This results in higher production costs and minimal flexibility in supporting multiple waveform standards. By contrast, software defined radio technology provides an efficient and comparatively inexpensive solution to this problem, allowing multi- mode, multi-band and/or multi-functional wireless devices that can be enhanced using software upgrades.

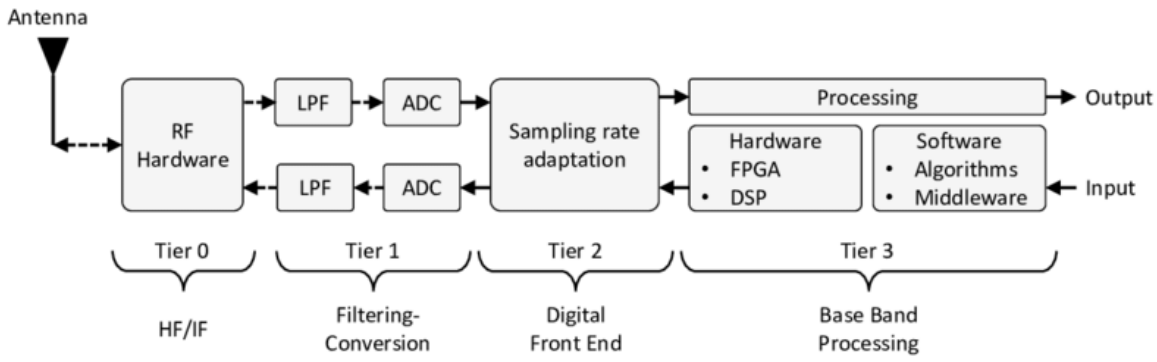

Figure 6: SDR Generalized Architecture.

3.3 DIGITAL FILTERING TECHNIQUES

Digital filters are used for two general purposes: (1) separation of signals that have been combined, and (2) restoration of signals that have been distorted in some way. Analog (electronic) filters can be used for these same tasks; however, digital filters can achieve far superior results[18].

Digital filters are a very important part of DSP. In fact, their extraordinary performance is one of the key reasons that DSP has become so popular. As mentioned in the introduction, filters have two uses: signal separation and signal restoration. Signal separation is needed when a signal has been contaminated with interference, noise, or other signals. For example, imagine a device for measuring the electrical activity of a baby's heart (EKG) while still in the womb. The raw signal will likely be corrupted by the breathing and heartbeat of the mother. A filter might be used to separate these signals so that they can be individually analyzed.

Signal restoration is used when a signal has been distorted in some way. For example, an audio recording made with poor equipment may be filtered to better represent the sound as it actually occurred. Another example is the deblurring of an image acquired with an improperly focused lens, or a shaky camera.

These problems can be attacked with either analog or digital filters. Which is better? Analog filters are cheap, fast, and have a large dynamic range in both amplitude and frequency. Digital filters, in comparison, are vastly superior in the level of performance that can be achieved[3].

This section contains introductory information about digital filter design[19]. Application of digital filters can be done without knowing or understanding much of the mathematics behind the filters. This section discusses general digital filter applications, standard terminology, design principles, and analysis techniques needed to design and analyze the characteristics of a digital filter.

Filters are signal processing elements that alter the frequency spectrum of an input signal. Filters might be applicable for the following applications:

- Attenuating noise in a signal where the noise power and signal power are concentrated at different frequencies. For example, use a notch filter to attenuate a 60 Hz powerline interference present in a signal.
- Extracting signal components from a signal that contains different signal components concentrated at different frequencies. For example, use a bandpass filter to extract a particular radio station signal from a received broadband radio signal.
- Reshaping the frequency spectrum of the input signal. For example, an A-weighting filter to approximate the frequency response of a human ear. As another example, an equalizer filter can be used to undo magnitude and phase distortion caused by passing a signal through a linear time-invariant communications channel.

Most commonly, fixed-point or floating-point arithmetic can be used to implement digital signal processing systems. Although floating-point implementations are typically easier to design, fixed-point implementations are often less expensive and more power efficient than floating-point implementations. Floating-point designs are typically appropriate in applications that run on desktop computers, and fixed-point designs are often more appropriate in embedded applications, in which it can be important to minimize cost or power consumption.

When designing a digital filter, we begin by creating specifications that define the characteristics we want in the digital filter. This section explains the characteristics of digital filters we create using the LabVIEW. The expected filter input signal is a series of discrete digital values. The set of discrete digital coefficients determines the filter frequency response. Digital filters have many advantages over analog filters. For example, the frequency response of digital filters generally does not depend on the parametric variation of electronic components or power supply noise or droop.

In a FIR (Finite Impulse Response) filter after an input is set to zero, the filter output signal can be non-zero for only a finite number of sample times before it also becomes zero. Whereas, an IIR (Infinite Impulse Response). The output signal from the filter can be non-zero infinitely after the input signal is changed from non-zero to zero. The choice between FIR and IIR filters affects both the filter design process and the implementation of the filter, as explained in the following sections.

One difference between FIR and IIR filters is the impulse response, which is finite or infinite, respectively. That difference alone is not likely to be important as you design a filter, but FIR and IIR filters have other differences that might affect the design. For example, FIR filter implementations typically require more multiplications and summations than IIR filters with similar filtering performance. However, because computer architectures are frequently better suited to performing FIR filtering, the computation speed of an IIR filter is not necessarily faster than a FIR filter. Table 1 compares the attributes of causal FIR and IIR digital filters.

Table 1: Comparison of FIR and IIR Filter.

Attribute	**FIR Filter**	**IIR Filter**
Linear Phase Response	Possible	Not possible
Stability	Always stable	Conditionally stable
Fixed-point conversion	Easy to implement	Can be complicated to implement

Computational complexity	More computations	Fewer Computations
Datapath precision typically	Less precision required	Greater precision required

LabVIEW provides several design methods, including Elliptic, Chebyshev, Inverse Chebyshev, and Butterworth, for IIR digital filters. Each design option offers different characteristics. For example, Butterworth filters characteristically have a smooth response at all frequencies and also are monotonically decreasing or increasing in the transition band. However, Butterworth filters do not always provide an acceptably accurate approximation of the ideal filter response because the filter has slow roll off in the transition band. If you need sharper roll off than a Butterworth filter can provide, use a Chebyshev, Inverse Chebyshev, or Elliptic design. Refer to the *LabVIEW Help* for complete reference information on the Filter Design VIs and different design methods.

The toolkit also provides several design methods, including the Kaiser Window method and the Remez algorithm, for FIR digital filters. The window-based methods are classical, while the Remez algorithm is complicated but provides optimal results.

The Filter Design VI automatically computes the minimal filter order required to fulfill the given filter specification and displays the order in the Filter Order indicator. Given the same specification, different algorithms design digital filters with different filter orders. You can estimate the computational complexity and cost to some extent based on the filter order. For strict requirements by the system, filter order can help us determine if the filter is acceptable.

For most digital filters, we typically design the digital filter response in the frequency domain. The frequency response specification for the digital filter typically includes the target magnitude response, phase response, and the allowable deviation for each. Figure 7 and Figure 8 illustrates a bandpass and bandstop filter specification respectively.

The following parameters must be defined in a filter specification: passband gain, maximum passband ripple, passband edge frequencies, stopband edge frequencies, and minimum stopband attenuation (alternatively, maximum stopband gain). The passband ripple defines the maximum allowable deviation δp from the desired passband gain. Minimum stopband attenuation indicates the maximum allowable deviation δs from zero stopband gain.

Notice the transition band between the passband and stopband frequencies. In an ideal design, a digital filter has the target gain in the passband and zero gain ($-\infty$ dB) in the stopband. In a real implementation, a finite transition region between the passband and the stopband, which is known as the transition band, always exists. The gain of the filter in the transition band is unspecified. The gain usually changes gradually through the transition band from 1 (0 dB) in the passband to 0 ($-\infty$ dB) in the stopband.

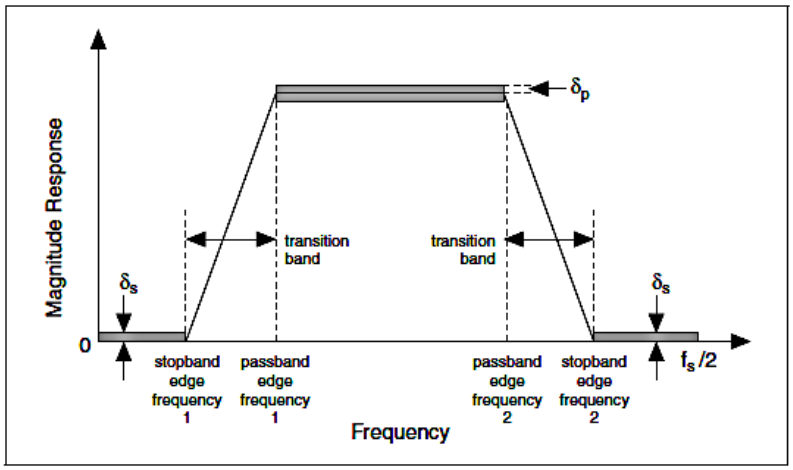

Figure 7: Bandpass filter response.

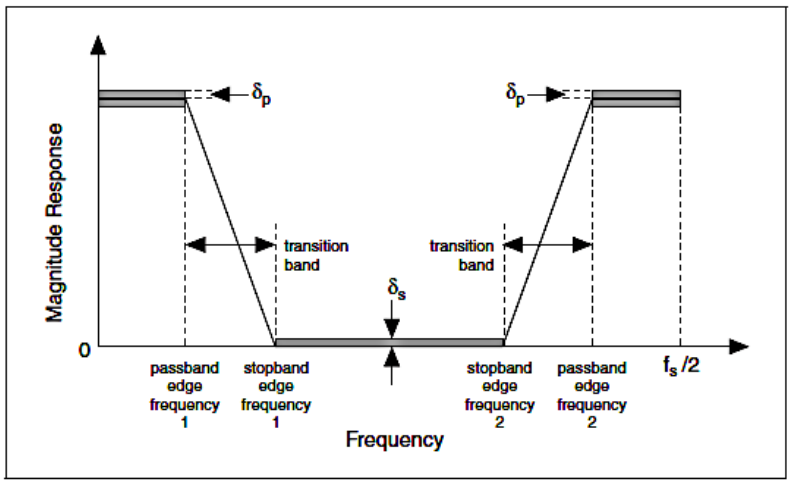

Figure 8: Bandstop filter response.

3.4 COGNITIVE RADIO

Cognitive Radios (CR) are smart radio systems that autonomously coordinate the usage of radio band. They can characterize and recognize radio spectrum when it is unused by the incumbent radio system and use this spectrum in an intelligent way. Such unused radio spectrum is called 'spectrum opportunity,' also known to as 'white space.'[20]. It was first stipulated by

Joseph Mitola III and Gerald Q. Maguire, Jr in 1999. This is an intelligent wireless communication system that is cognizant of its surrounding environment and uses a understanding methodology by building to learn from the environment, adapt its internal states to statistical change in the incoming radio frequency stimuli by making corresponding variation in certain operating parameters in real time and with two primary objectives: i) highly reliable communications whenever and wherever needed ii) efficient utilization of radio spectrum.

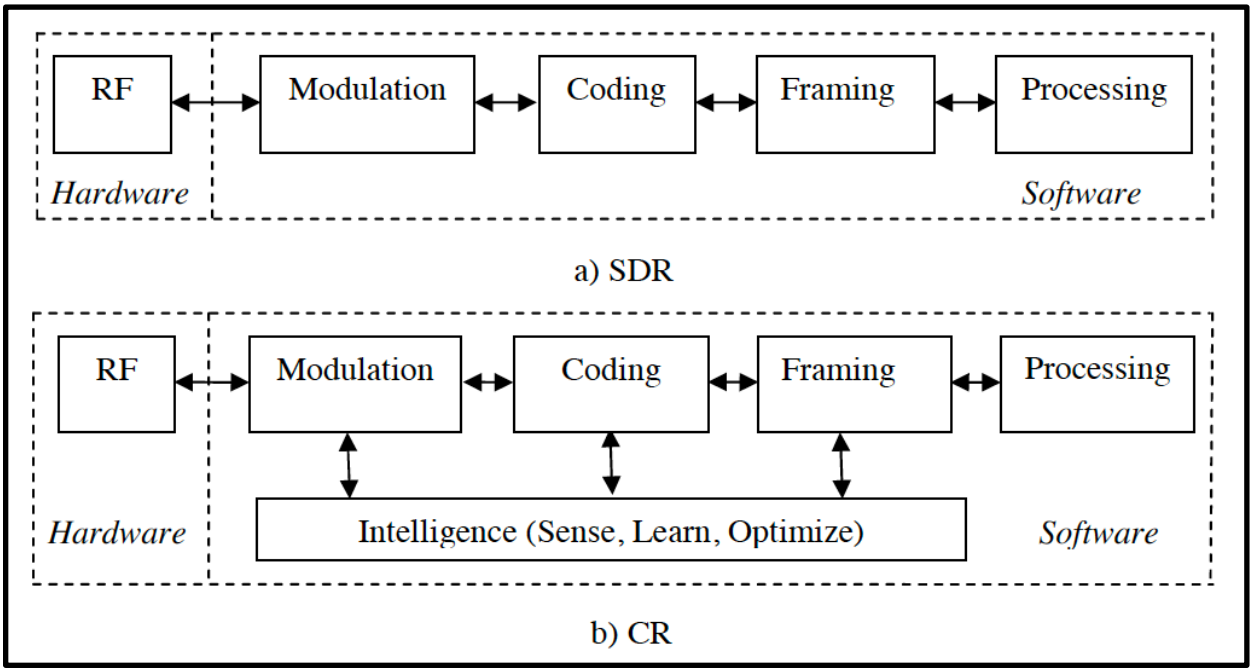

Figure 9: CR implementation in a SDR

The functions of a Cognitive Radio can be categorized with specific functions. For example, spectrum sensing determines if a primary user is present on a band. The results of detection are shared among different cognitive radios. Spectrum management plays a vital role by deciding on the best band of the spectrum to ensure Quality of Service (QoS) of the radio link. It encompasses the spectrum analysis based on the Signal to Noise Ratio (SNR), the average correlation and the availability of the white spaces. In an environment where co-ordination is

necessary there needs to be a decision-making unit like a controller to ensure uninterrupted spectrum access. When CR users switch between frequency bands which are not allocated for them, a handoff mechanism needs to be established for mobility. Spectrum scheduling are achieved by allowing secondary users to use available spectrum holes efficiently and selflessly [21].

Dynamic Spectrum Access (DSA) is the most significant application of CRs. A technique by which a radio system adapts to available spectrum holes with limited spectrum use rights dynamically, in response to changing circumstances and objectives: the created interference changes the radio's state in environmental constraints. The main task of DSA is to overcome two types of interference: i) harmful interference caused by device malfunctioning and ii) harmful interference caused by malicious user [22]. The main functions of the DSA are Spectrum awareness, cognitive processing and spectrum access. Among various methods of DSA approach, Markovian Queuing Model is the one which uses the centralized architecture with a central controller allocating bandwidth to the users. This model provides a good compromise between accuracy and computation complexity.

Chapter 4: Methodology

This section will layout the experimental design to generate RF signals and analyze the interference scenario. The Universal Software Radio Peripheral (USRP) will be programmed to generate RF signals and study the interference between adjacent radio frequency signals.

4.1 Testbed Layout

The preliminary layout of the experiment that will be used to recollect data is depicted in Figure 10. The purpose of the blocks is to ensure a basic communications system with added interference. The telemetry and LTE systems are generated from simulation. The telemetry system will be the primary user and facing interference from the LTE system, in order to observe the behavior of these two systems in conjunction. A second test will be performed to compare LTE as the primary user and the telemetry system as a source of interference.

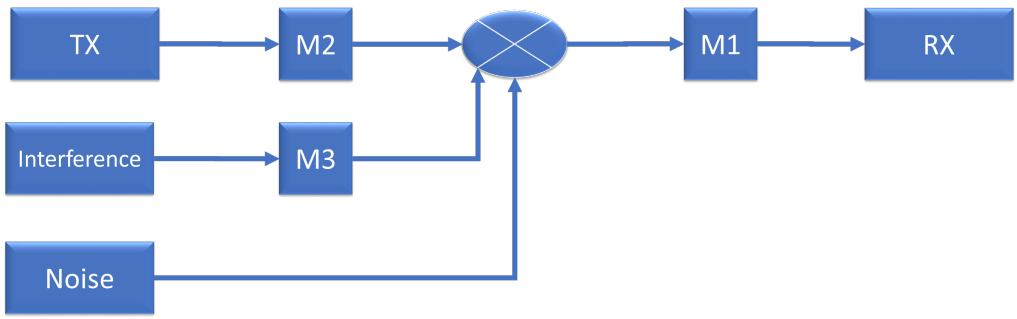

Figure 10: A basic layout of the communication system.

The system blocks in Figure is composed of hardware device with a specific assignment. TX and RX represents the primary user's system, either telemetry or LTE. The three M blocks are mitigation devices which can be manipulated by the controller. Interference and Noise source are included to test the performance of the whole system under stress.

The telemetry will be the initial transmitter (TX) and receiver (RX) with the interference being the LTE system. Later they will be interchanged, meaning telemetry being the interference on the LTE system for experimental purposes. Additive white gaussian noise (AWGN) is considered as the Noise source. A mixer will add all the signals, represented by a cross in the circle to be received by RX. The accuracy of the received data will be achieved using the mitigation blocks (M1, M2 and M3). Signals will be analyzed based on the adjustable parameters: frequency, modulation (PSK, QAM etc.), power (dB/dBm), and bandwidth. The carrier frequency will be static, whereas power from the transmission source TX, Interference, and noise will be variant.

The mitigation blocks will include attenuators, filtering solutions for experimental purpose. The end goal is to achieve a zero value for Frame Synchronization Error Rate (FSER) obtained from the telemetry system. To avoid any FCC violation closed loop experiments will be performed in various bands. The parameter values will be close to the actual values used by the real-world equipment, in this case WSMR equipment.

4.2 IMPLEMENTATION

With the goal of building a cognitive radio testbed based on the SDR platform all the components were acquired. This includes SDRs, coaxial cables, splitters and combiners. Telemetry signals were generated using one of the SDRs with several PSK modulation schemes. The interference source LTE required two SDRs for uplink (UL) and downlink (DL) transmission by the user equipment (UE) and eNodeB (eNB) respectively. The remaining SDR was used for the AWGN source. All of these is combined in a final SDR assigned for filtering which will yield a clean Telemetry signal

A spectrum analyzer is placed before the filter and another after the filter to observe the changes and quality of signal that is filtered out. The complete testbed is depicted in Figure 11 with the devices labeled for simplicity.

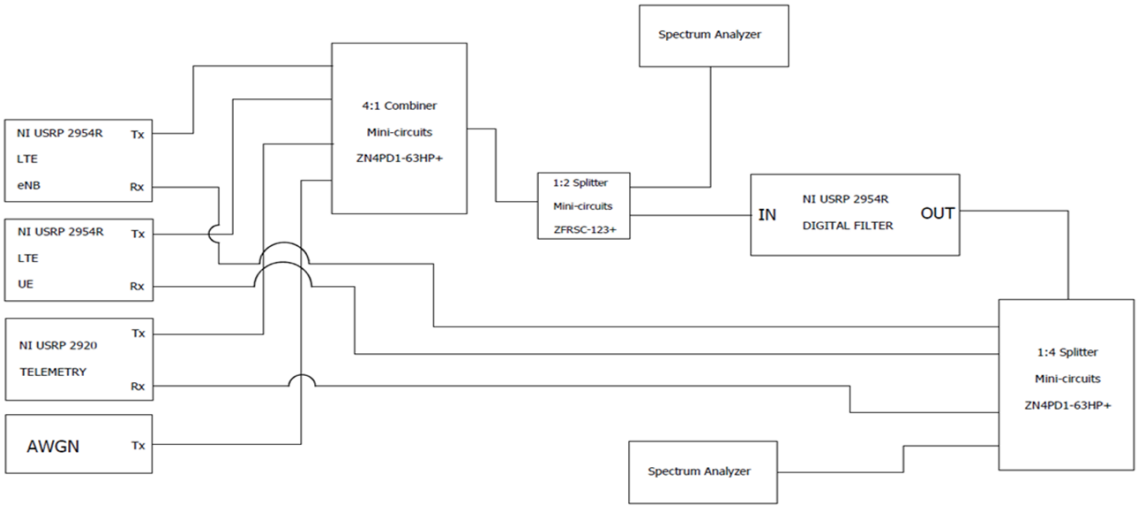

Figure 11: The final testbed with the Telemetry, LTE interference, Noise, digital filter and spectrum analyzers.

The physical testbed is shown in Illustration 1, with SDRs and cables connecting them to the splitters and combiners. The SDR for filtering is shown in Illustration 2 and the spectrum analyzers used to detect signals before and after filtering shown in Illustration 3.

Illustration 1: The SDRs with transmitters and receivers along with splitters and combiners.

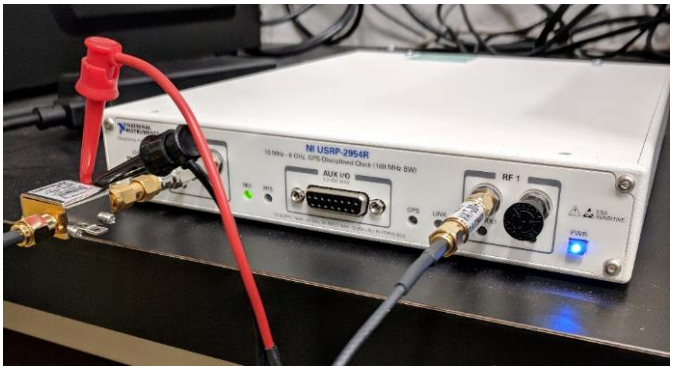

Illustration 2: SDR utilized for filtering.

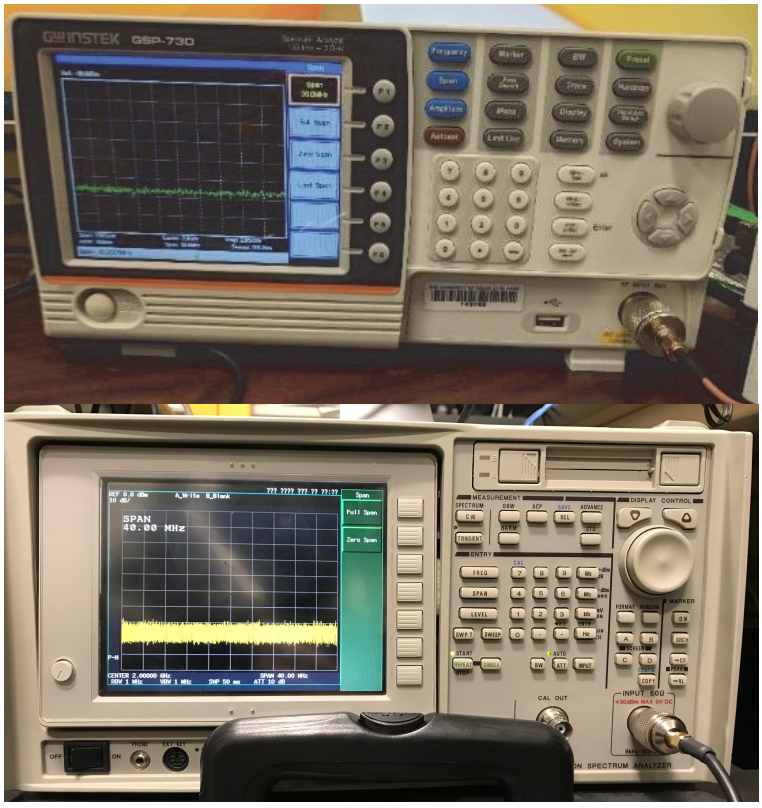

Illustration 3: Spectrum analyzer for pre (on top) and post (on the bottom) filtered signal detection.

4.2.1 Numerical Parameters from Testbed

To quantify the performance of the system, numerical parameters must be obtained. These parameters will be obtained in the border regions between the telemetry and the LTE frequency bands. It is important to notice the performance in different frequency bands to see how they differ depending on what frequency band they are in (if any).

The numerical parameters include: antenna gain G/t, Bandwidth (BW) of the transmitted signal, BER or BLER (in LTE systems) typically required to be ≤ 10^(-6), center frequency (fc) in Hz, data rate in mbps, frame synchronization error rate (FSER) most likely required to be zero, I/Q rate, modulation scheme, noise floor can be calculated by the input SNR vs output SNR when

passing through a device or by output noise vs thermal noise, Rx power in dB, Rx sensitivity level (detection threshold), SNR and Tx Power.

All these quantifying parameters are to be obtained in the frequencies of interest, while focusing mainly on the telemetry frequencies and their border bands.

4.2.2 Visual Parameters from Testbed

To qualify the performance of the system, visual parameters must also be obtained along with the numerical parameters. In every of the tests performed for the numerical parameters, the visual parameters have to be observed —mainly through a spectrum analyzer or a Vector Network Analyzer (or any of its variations)— to ensure that the system is working as expected. Several images are included in this section in order to compare them to what the visual devices are outputting. They were generated using the testbed in study by using a BPSK signal. A clean signal vs. a noisy signal is shown for each of the parameters described below.

The visual parameters include typical constellation in Figure 12, eye diagram in Figure 13 and FSER and data rate in Figure 14.

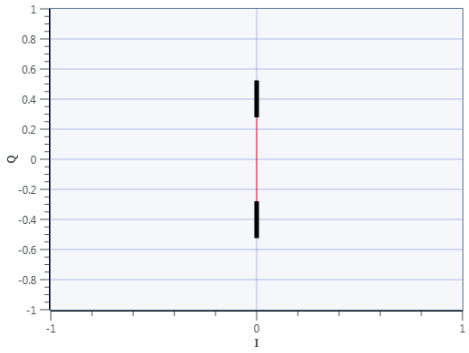

Figure 12: Constellation Diagram for a BPSK signal (rotated 90° for illustration purposes). This image was generated using the testbed.

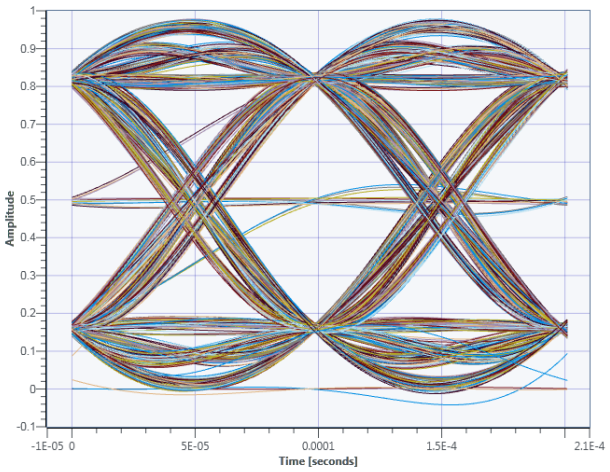

Figure 13: A PSK eye diagram. Generated only for illustration purposes.

These results are useful to help classify the testbed and the experiments in a numerical and visual way. Compliance values are usually set by the consumer, although the main values of concern are the Tx power, FSER, data rate, and SNR. Again, these values will help classify the performance of the experiment scenario.

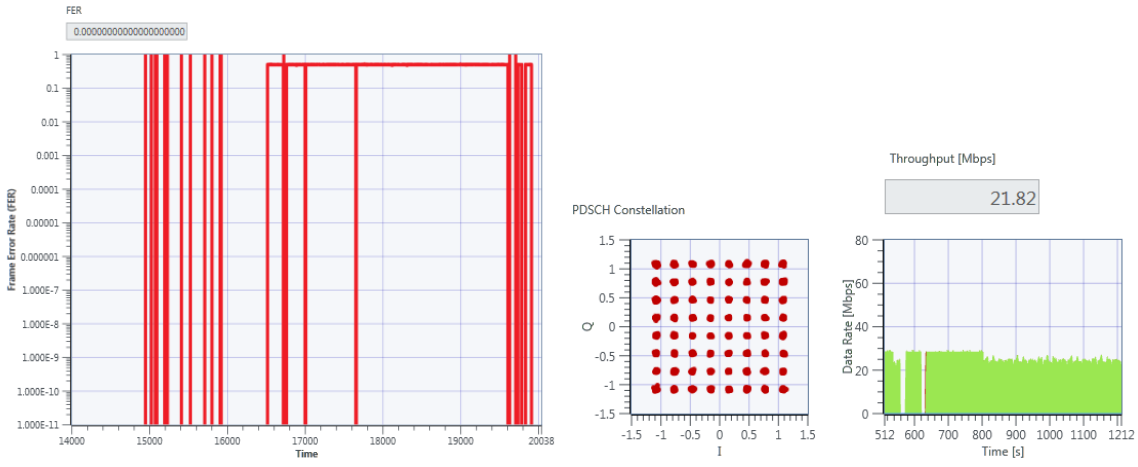

Figure 14: FSER and data rate measurements.

Eye diagrams, constellation diagrams, and spectrum graphs can be obtained from the laboratory experiments. With the qualitative and quantitative results, the rules and techniques of interference mitigation can be generated.

4.3 EXPERIMENTATION

After performing several experiments, the results are presented in Chapter 5. The telemetry (TM) and LTE systems were simulated in out of band, adjacent band and in band to study the interference scenario. Two different modulation schemes were used for the TM and LTE systems, they are OQPSK and 64-QAM respectively. Both of them are aggressive modulation schemes, used for the purpose of worst-case scenario.

Adjacent band experiments were done in the Upper L and Lower S bands with the TM frequency centered at 1780 MHz and LTE UL frequency centered at 1786 MHz. In the second case, TM frequency was centered at 2215 MHz and LTE DL frequency centered at 2200 MHz which were adjacent to each other. These experiments gave us the idea of actual adjacent band scenario with the ideal guard band required between two signals.

Next set of experiments were done in out of band, meaning the TM and LTE frequencies set at the center of their designated spectrum bands further away from each other. Initially TM was centered at 1850 MHz and LTE UL at 1767MHz. Afterwards, TM was centered at 2245 MHz and LTE DL at 2167 MHz. These experiments were considered to be the baseline depicting minimal interference from TM on LTE systems and vice versa.

The last set of experiments were done to observe the in band transmission from TM and LTE systems which is unlikely to happen. Both TM and LTE UL frequencies were centered at

1780 MHz, also TM and LTE DL centered at 2200 MHz. This resulted in overlap of the signals from both the system. The bandwidth of LTE signal is 20 MHz, and TM signal is typically 200 kHz.

In order to explore the digital filtering techniques in mitigating interference between adjacent radio frequency signals, experiments were done in narrowband with amplitude modulated signals. A simple setup with the SDRs will analyze digital filtering with different types of IIR filter and their order. The filtering techniques using several IIR filters: Butterworth, Chebyshev and Elliptic are among the popular ones. Signals are transmitted in adjacent bands in order to study the performance of the bandpass rejection filters.

Amplitude Modulated (AM) signals are mixed using Frequency Division Multiplexing (FDM) method before transmission shown in Figure 15. Bandpass filter (BPF) in the receiver (RX) removes the interfering signal depending on the frequency response of the designed filter. The stopband and passband frequencies and their ripples of the BPF are adjustable. NI USRP SDRs were programmed using LabVIEW Communications Design Suite 2.0 to design the following transceiver.

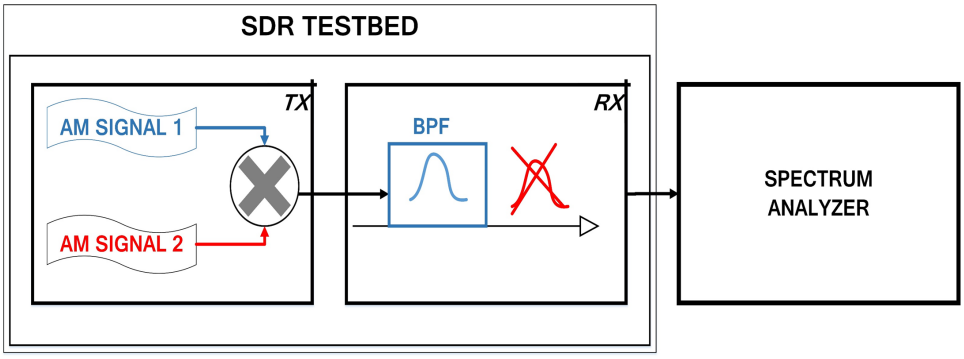

Figure 15: Testbed to analyze the performance of BPF.

A spectrum analyzer is included to observe the filtered output waveform. Laboratory experiments were conducted using Butterworth, Chebyshev and Elliptic filter with variable filter orders in the narrowband with the AM signal 1 centered at 500 kHz and AM signal 2 centered at 501 kHz.

The transmitter (TX) carrier frequency is set at 915 MHz with subcarrier frequencies at 500 kHz and 501 kHz for AM signal 1 and AM signal 2 respectively. The TX gain is set to zero dB with I/Q rate typically 2 millions, and samples typically 200,000.

The receiver (RX) was configured with the same carrier frequency, gain, I/Q rate and sample values as the TX. Additionally the RX was equipped with a BPF having the adjustable parameters: low cutoff frequency in Hz, high cutoff frequency in Hz, filter order, passband and stopband ripples as shown in Figure 16.

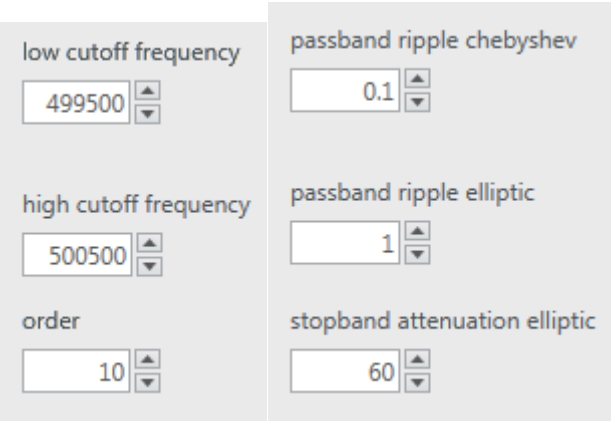

Figure 16: BPF filter inputs.

4.4 COMPUTATIONAL METHODS

The AM signals generated with the LabVIEW building block can also be done computationally with the help of Mathscripts integrated in LabVIEW. This section contains communication scheme known as frequency division multiplexing, which is implemented using Mathscript, the signal processing operations necessary to receive the transmitted sinusoid signals. The results are demonstrated in chapter 5.

Frequency Division Multiplexing (FDM) is a communication scheme that allows multiple information signals to be sent simultaneously across a communication channel. FDM assigns to each information signal a frequency band within the communication channel's spectrum. Since the frequency bands are chosen so they don't overlap, the information signals travel through the channel without interference. Figure 17 illustrates the transmission of two information signals using FDM.

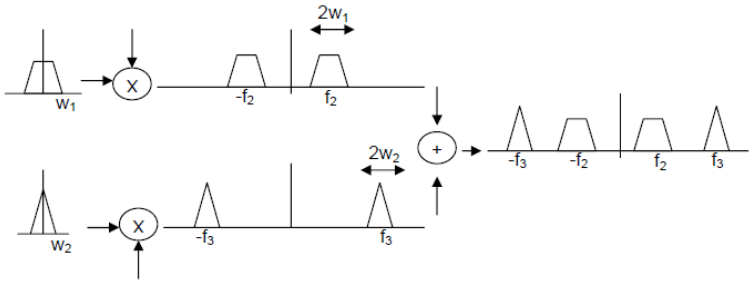

Figure 17: Frequency division multiplexing.

In Figure 17 two information signals with spectra shaped as a trapezium and a triangle respectively. To send these information signals simultaneously over the same communication channel using FDM, we *modulate* each of the information signals to a different frequency band. In this example, we modulated the information signal corresponding to the trapezium spectrum to a frequency band with center frequency f_2 and bandwidth w_1; and we modulated the information signal with the triangular spectrum to a frequency band with center f_3 and bandwidth w_2. By

adding these two modulated information signals we obtain a *transmission signal* that can carry the spectra of both information signals across the communication channel simultaneously.

At the receiver the transmission signal must be processed in order to extract the information signal of interest. This processing involves removing the unwanted spectral components from the transmission signal, and then demodulating the spectral component of interest back to DC (0Hz). As an example, Figure 18 illustrates the processing steps necessary in order to extract the information signal with the trapezium spectrum.

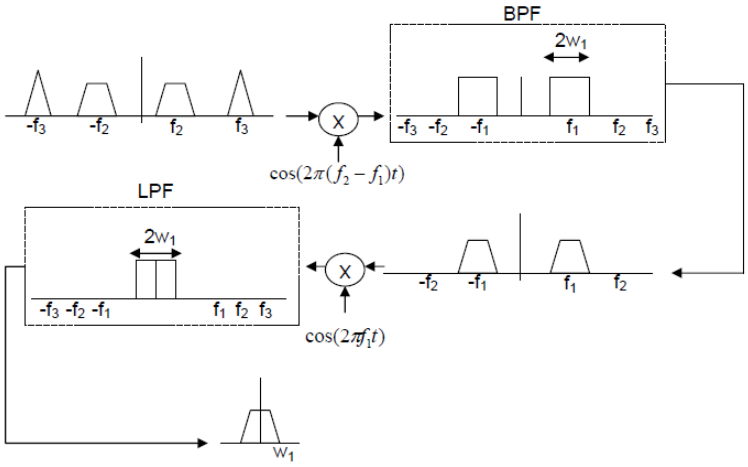

Figure 18: Steps for extracting information signal with trapezium spectrum.

First the transmission signal is modulated so that the spectral component of interest is positioned at the center frequency of a bandpass filter; in this case the trapezium spectrum is shifted so that it is centered at f_1. The bandpass filter keeps only the spectral components of the information signal of interest (the trapezium) and removes the spectral components corresponding to the second information signal (the triangle).

Next, the trapezium spectrum is demodulated to DC (the original center frequency of the information signal spectrum) and low pass filtered in order to remove the higher frequency

demodulation products (at $2f_1$ and $-2f_1$). The result is the information signal with the trapezium spectrum.

The same process is used to extract the information signal with the triangular spectrum except now the receiver modulates the received signal by $cos(2\pi(f_3 - f_1)t)$ as opposed to $cos(2\pi(f_2 - f_1)t)$. Modulation by the $f_3 - f_1$ frequency cosine centers the triangular spectrum at f_1. Now when the bandpass filter is applied only the spectral components of the information signal of interest (the triangle) are kept. The steps necessary to extract the triangular spectrum are illustrated in Figure 19.

The receiver just discussed is known as the superheterodyne receiver. It was developed by Edwin Armstrong in 1918. The main advantage of the superheterodyne receiver is that it allows the majority of the processing blocks of a radio receiver to be designed and operated at a narrow, low frequency range ($[f_1 - w_1\ f_1 + w_1]$ as opposed to operating in a wide, high frequency range ($[f_2 - w_1\ f_3 + w_2]$). Designing high performance processing blocks that operate in a narrow, low frequency range is far easier than designing processing blocks to operate in a wide, high frequency range.

In summary, the key step in receiving an information signal from a frequency division multiplexed transmission signal is selection of the modulation frequency at the receiver that will center the spectrum of the information signal of interest in the passband of the bandpass filter.

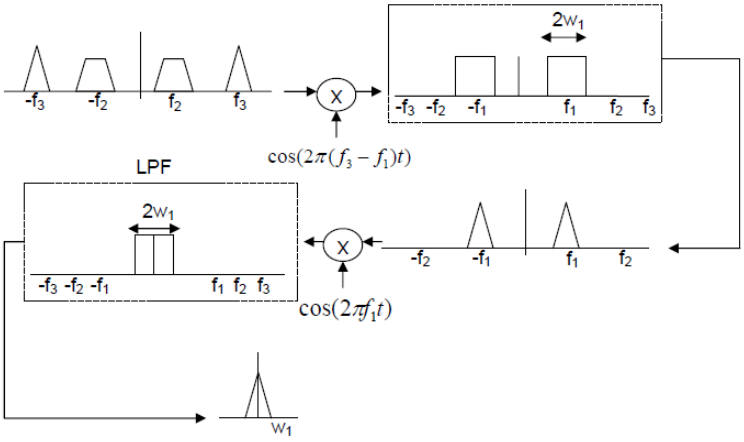

Figure 19: Steps for extracting information with triangular spectrum.

Chapter 5: Results

In this section the experimental results produced using the SDR testbed is demonstrated. The interference level from TM and LTE systems were measured for qualitative and quantitative analysis. The performance analysis of narrowband digital filter is also demonstrated. Later in the chapter, some computational methods are also demonstrated to generate RF signals using Mathscripts in LabVIEW without the signal processing blocks.

FSER, eye diagrams, constellations diagrams and power spectrum graphs were obtained from a set of experiments that included the adjacent band, out of band, and in band scenarios. The center frequency was changed in order to study these scenarios and the results were used to set rules for interference mitigation.

5.1 Baseline of TM and LTE System

The experimental results from the out of band scenario helped us to baseline the TM and LTE system performance since they were further apart from each other unlike the adjacent band or in band case. First, the results from the TM system in the bands 1815 MHz and 2245 MHz were observed, and finally the LTE UL in 1767 MHz and LTE DL in 2167 MHz

5.1.1 TM System Baseline

The modulation scheme used for the TM system was OQPSK with the center frequency at 1815 MHz and a gain of 10 dB. The power spectral density and the constellation graph is shown in Figure 20. Since there were no adjacent interfering signal, the TM RX constellation, power spectrum and the eye diagram were clean as depicted in Figure 21. This resulted in perfect zero FSER in Figure 22.

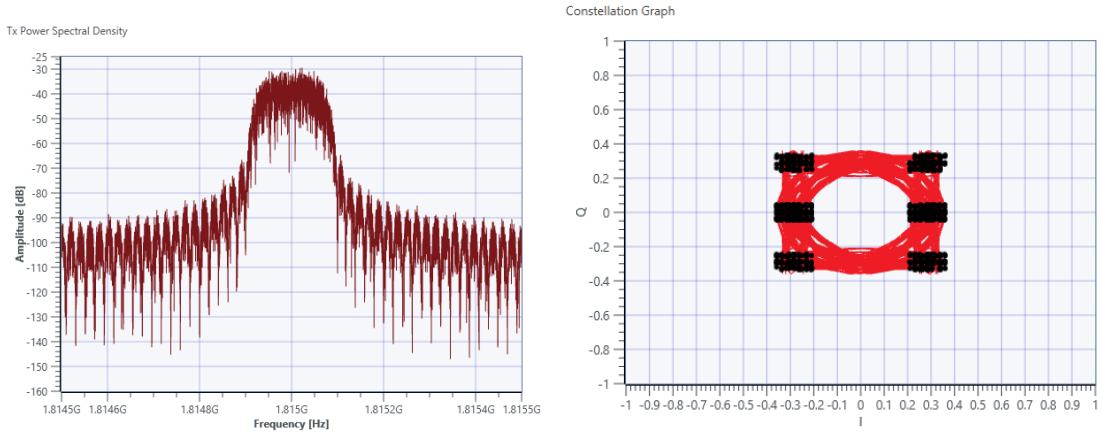

Figure 20: TM TX system power spectrum and constellation at 1815 MHz.

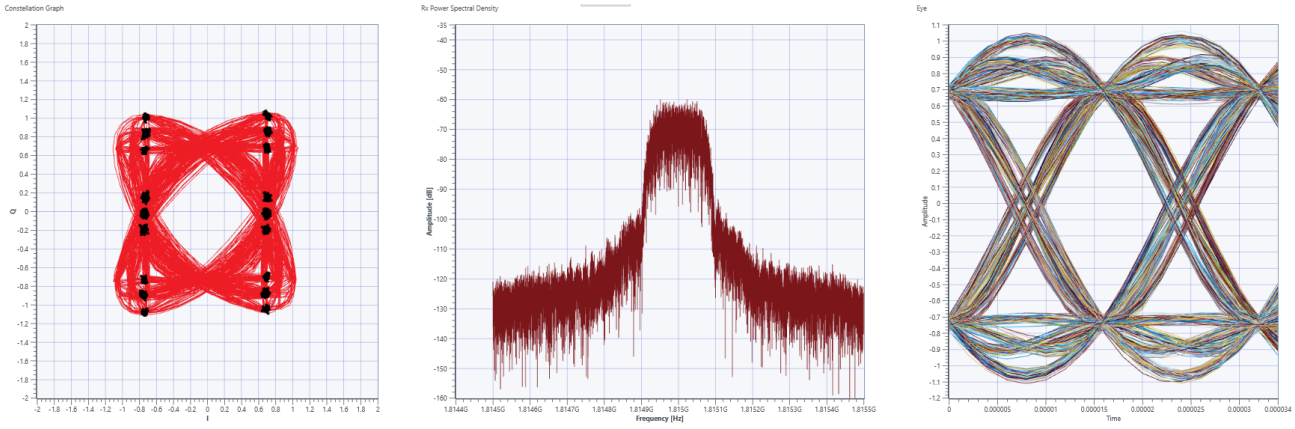

Figure 21: TM RX constellation, power spectrum and eye diagram at 1815 MHz.

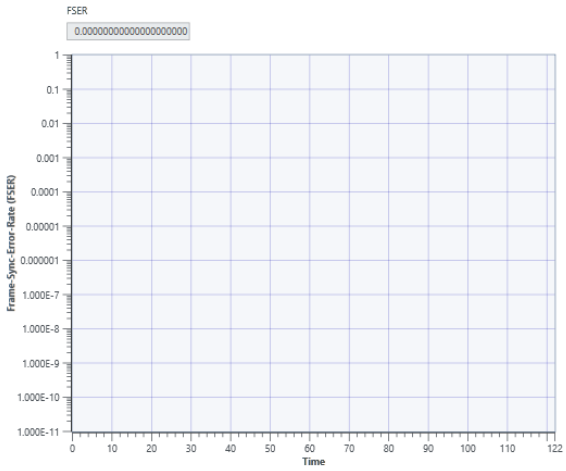

Figure 22: TM RX FSER at 1815 MHz.

The TM TX parameters were kept same with the center frequency changed to 2245 MHz close to the LTE DL system. The results were similar and are depicted in Figure 23, Figure 24, and Figure 25.

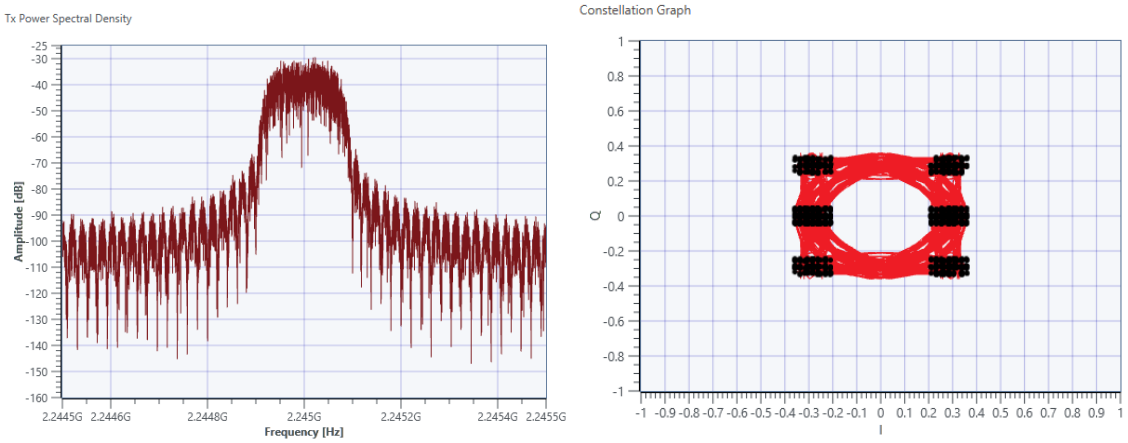

Figure 23: TM TX system power spectrum and constellation at 1815 MHz.

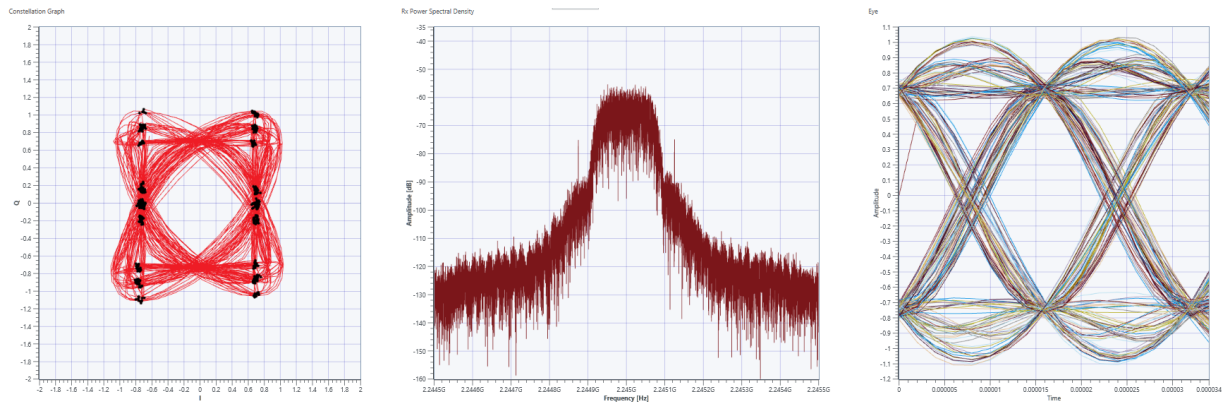

Figure 24: TM RX constellation, power spectrum and eye diagram at 2245 MHz.

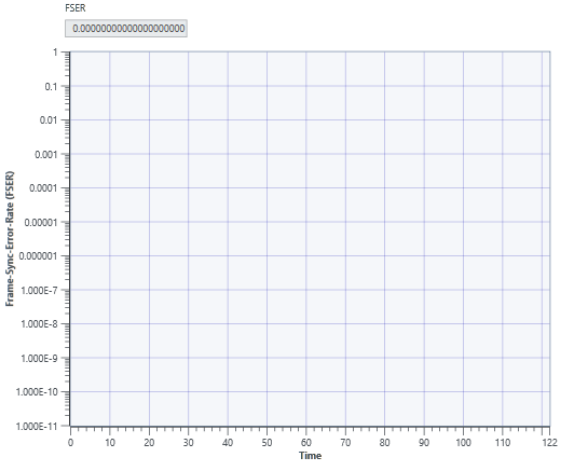

Figure 25: TM RX FSER at 2245 MHz.

5.1.2 LTE System Baseline

A 64-QAM modulation scheme was used for the LTE system. The LTE UL was centered at 1767 MHz with the power spectrum and the block error rate in Figure 26. The LTE DL frequency was centered at a higher frequency of 2167 MHz shown in Figure 27. The LTE system constellation and the data rate are shown in Figure 28. These results were taken for baseline purposes of the LTE system.

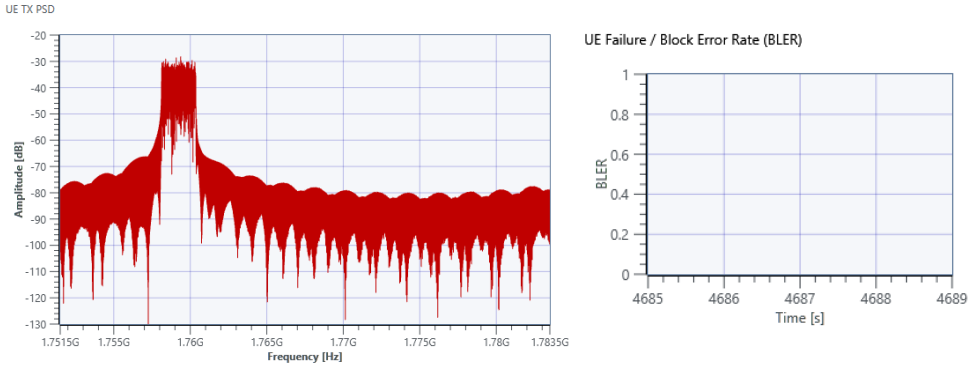

Figure 26: LTE UL power spectrum and BLER at 1767 MHz.

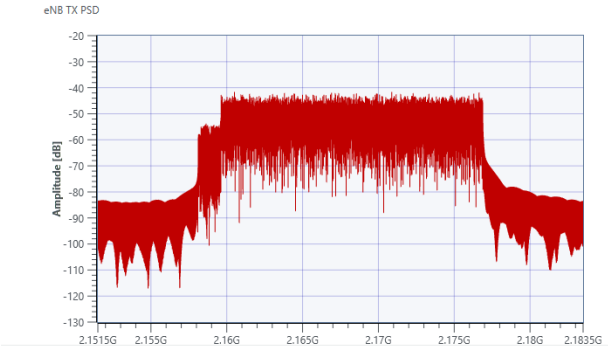

Figure 27: LTE DL power spectrum at 2167 MHz.

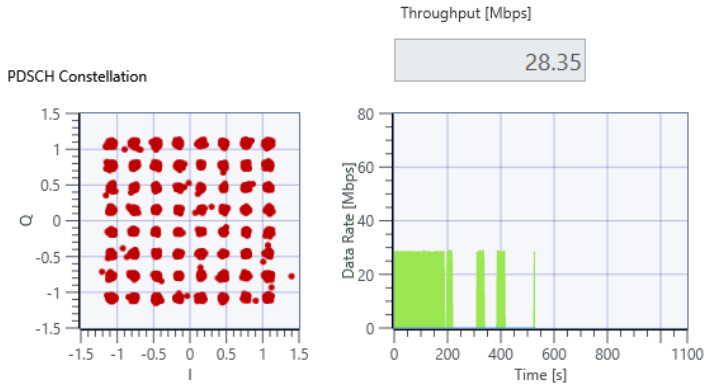

Figure 28: LTE system constellation and data rate.

5.2 LTE INTERFERENCE ON TM

The impact of LTE system on the TM system in the adjacent band and in band were observed with the FSER, constellation, power spectrum and eye diagram. The adjacent band included the TM frequency centered at 1780 MHz with LTE UL frequency centered at 1776 MHz, and TM frequency centered at 2215 MHz with the LTE DL frequency at 2200 MHz. The in band scenario included the both the system operating in the same frequency that is at 1780 MHz and 2200 MHz.

TM at 1780 MHz and LTE UL at 1776 MHz

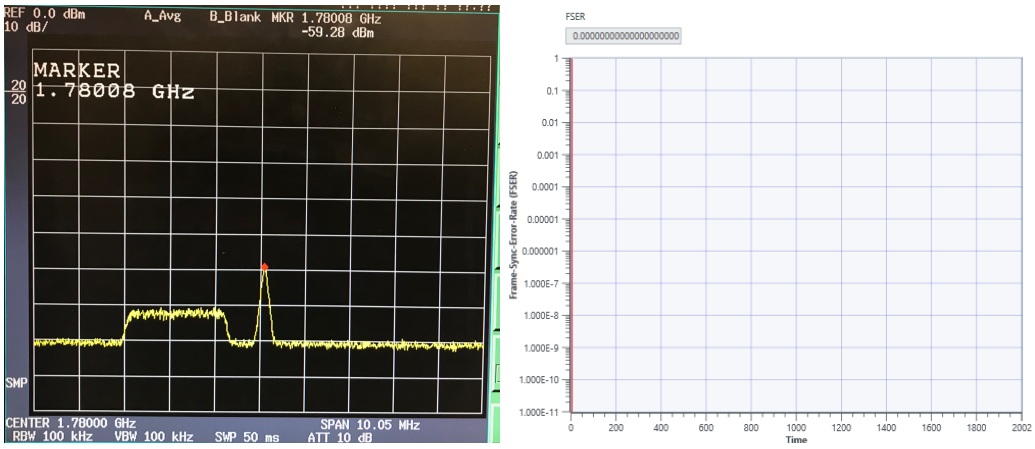

Figure 29: TM at 1780 MHz and LTE UL at 1776 MHz

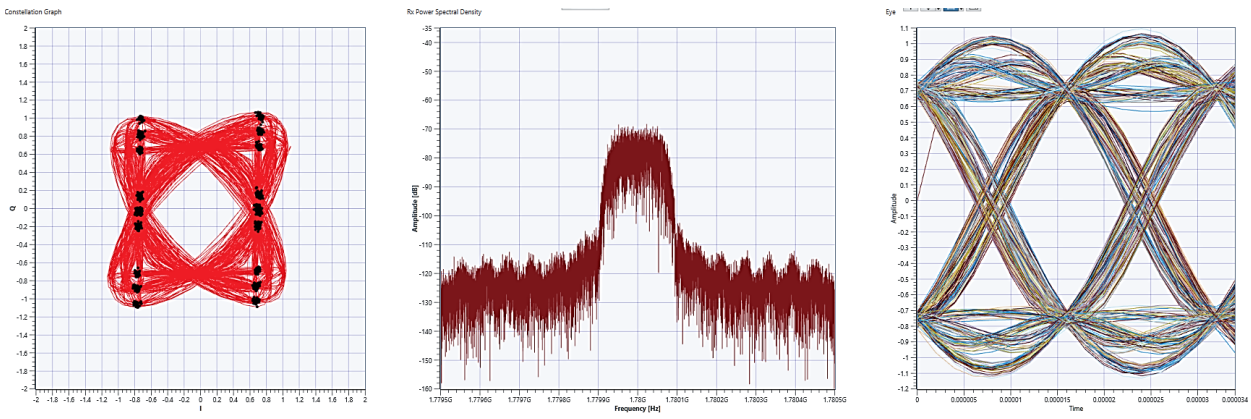

Figure 30: The constellation graph, power spectrum and the eye diagram at 1780 MHz.

TM at 2215 MHz and LTE DL at 2200 MHz

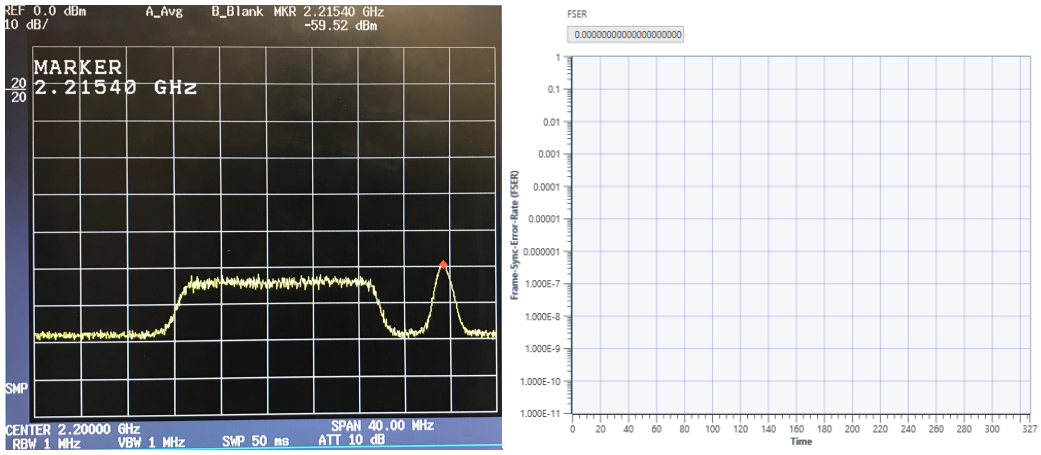

Figure 31: TM at 2215 MHz and LTE DL at 2200 MHz with FSER.

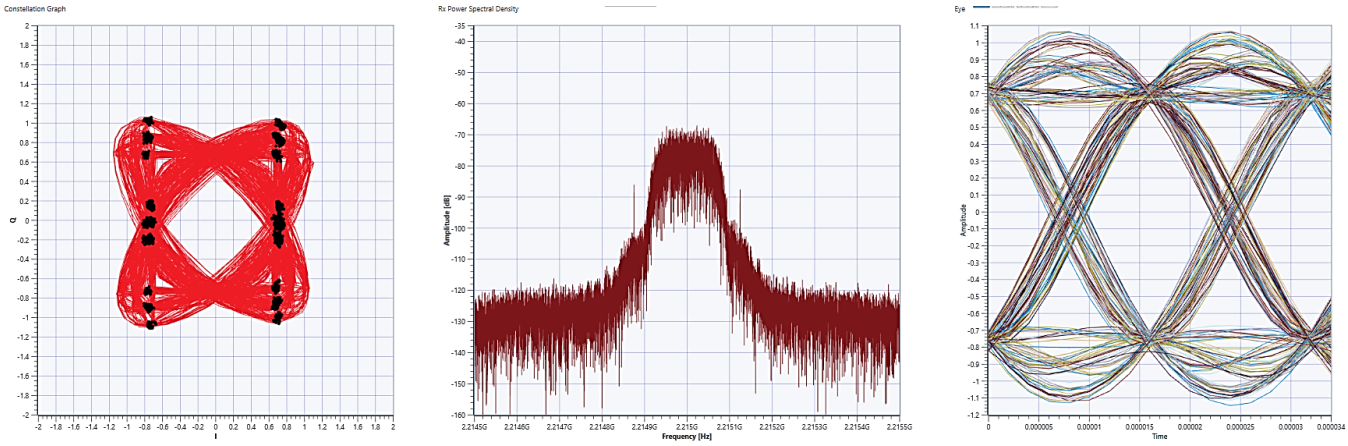

Figure 32: The constellation graph, power spectrum and the eye diagram at 2215 MHz.

The TM system was operational with the LTE UL and LTE DL system in the adjacent bands. The FSER values remained at zero with a clean constellation graph and eye diagram.

TM and LTE UL both at 1780 MHz

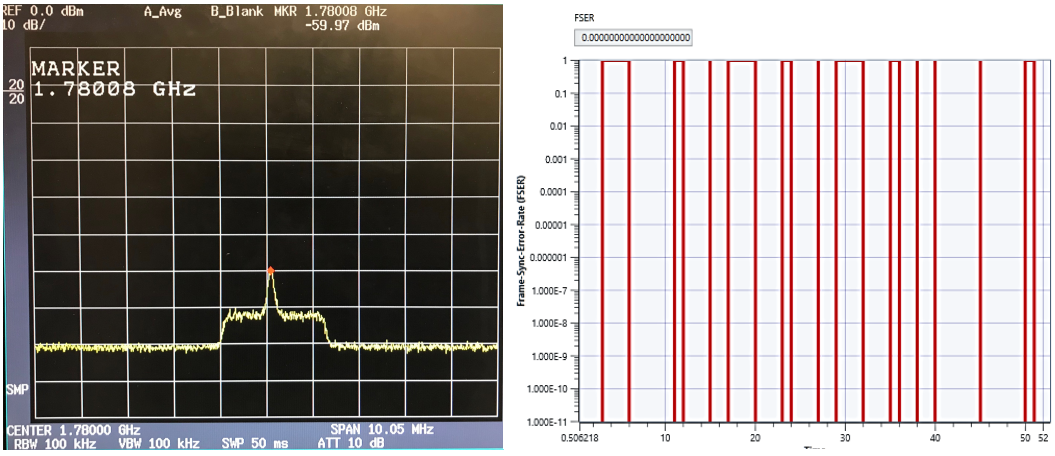

Figure 33: TM and LTE DL both at 2200 MHz with FSER.

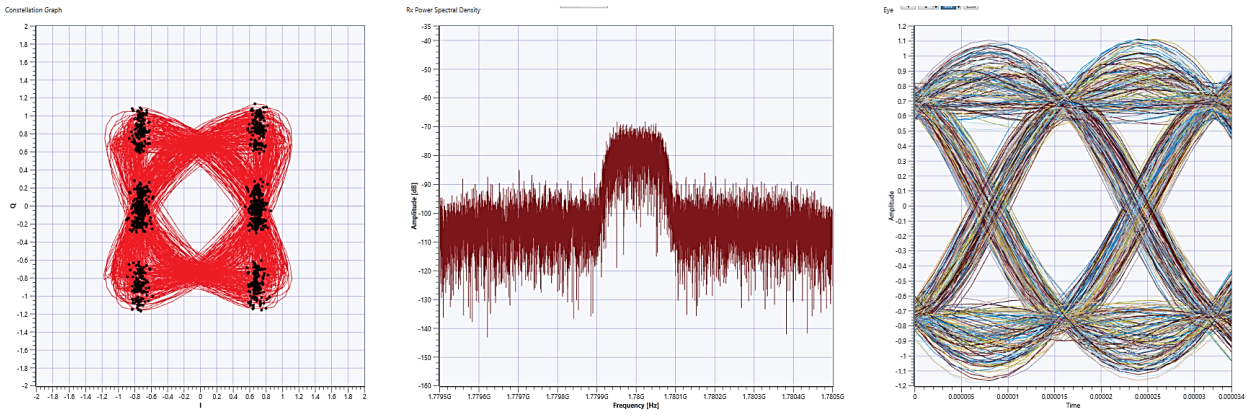

Figure 34: The constellation graph, power spectrum and the eye diagram at 1780 MHz.

TM and LTE DL both at 2200 MHz

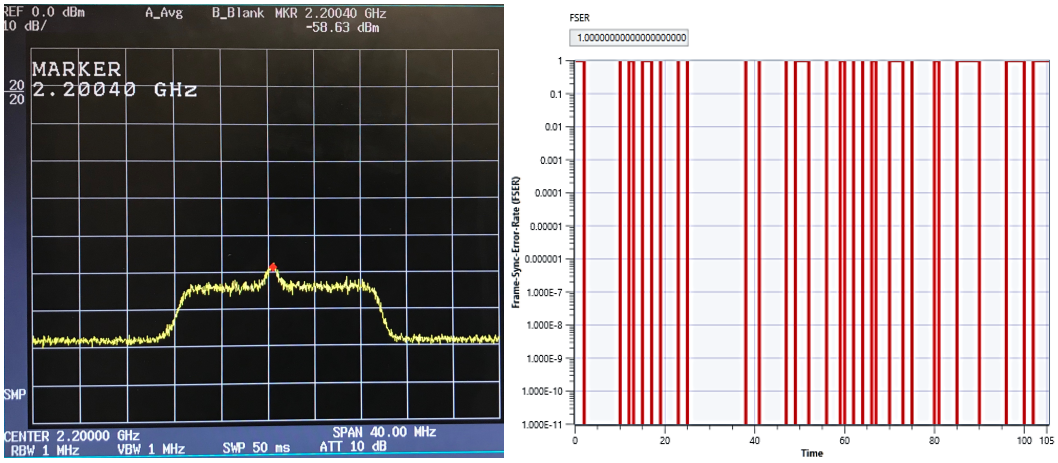

Figure 35: TM and LTE both at 2200 MHz with FSER.

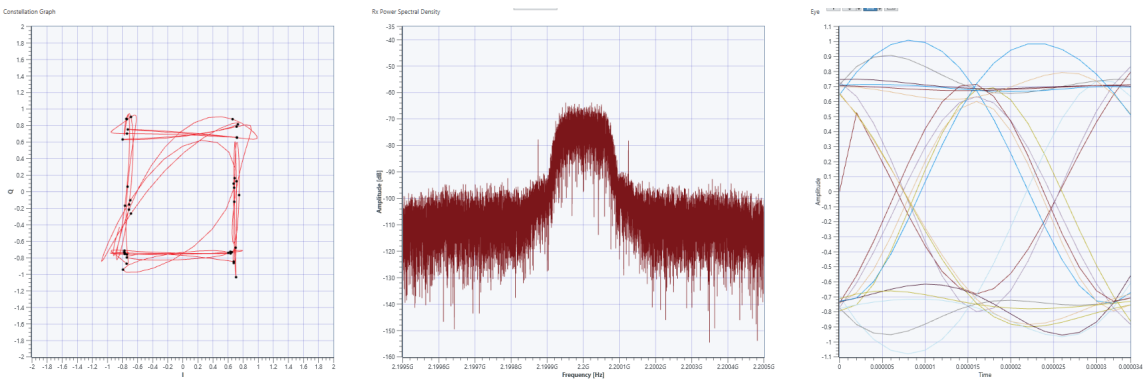

Figure 36: The constellation graph, power spectrum and the eye diagram at 2200 MHz.

The TM system was severely affected with the LTE system in the same band. The TM system performance at 1780 MHz was degraded with the constellation graph and eye diagram being jittery, and there is a drop in RX signal power with the FSER being highest due to the interference from LTE UL. The performance was much worse in the 2200 MHz with the TM system completely nonoperational due to the interference from the LTE DL.

5.3 TM INTERFERENCE ON LTE

The impact of TM system on the LTE system in the adjacent band and in band were observed with the performance parameters: BLER, constellation graph (PDSCH), and the data rate. The TM system, LTE UL and LTE DL system were centered at the same frequencies that were used for LTE interference on TM system previously.

LTE UL at 1776 MHz and TM at 1780 MHz

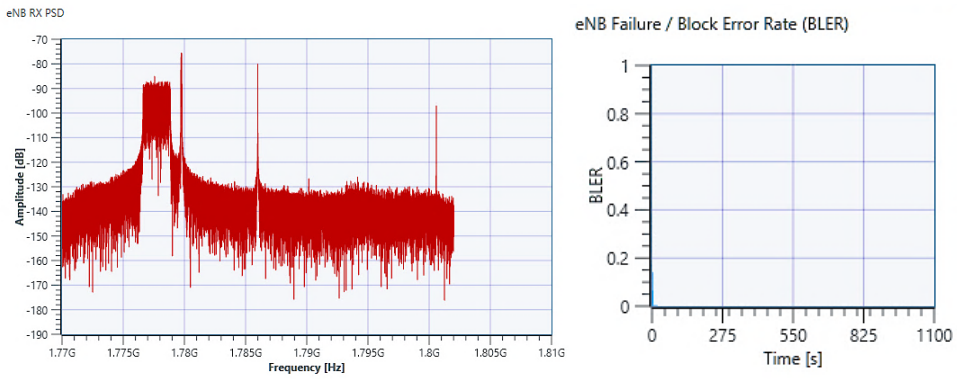

Figure 37: LTE UL at 1776 MHz and TM at 1780 MHz with the BLER.

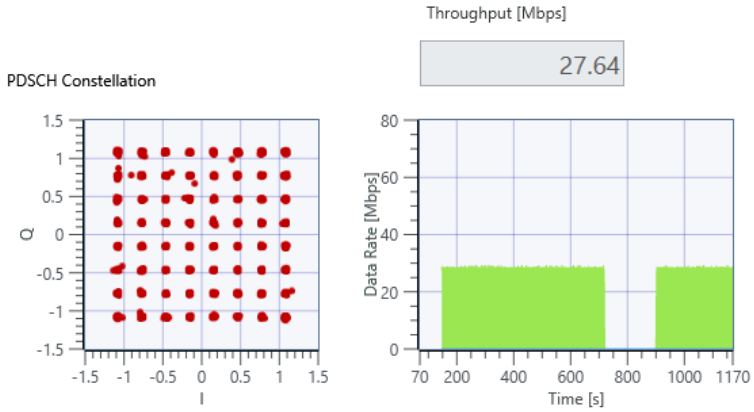

Figure 38: LTE UL constellation and data rate at 1776 MHz.

LTE DL at 2200 MHz and TM at 2215 MHz

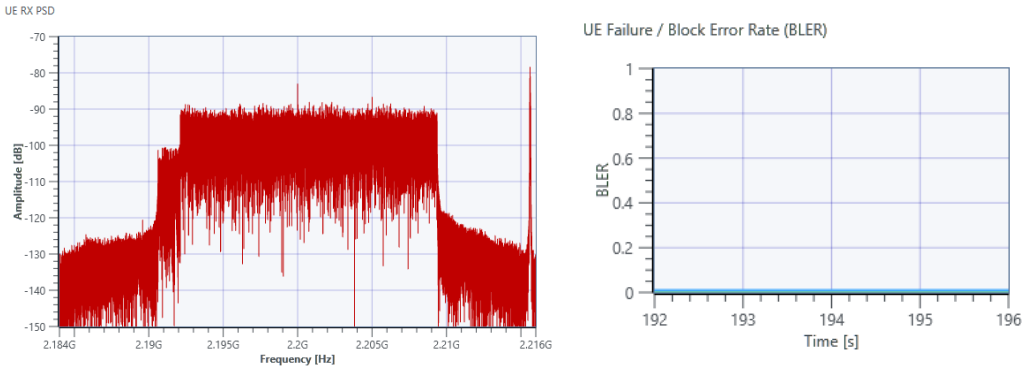

Figure 39: LTE DL at 2200 MHz and TM at 2215 MHz with the BLER.

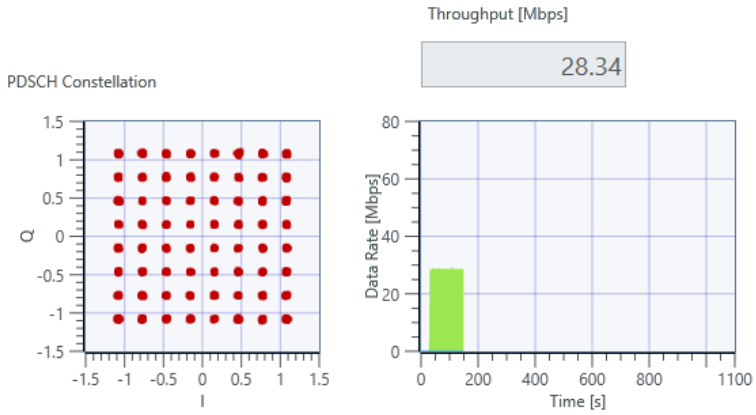

Figure 40: LTE DL constellation and data rate at 2200 MHz.

The performance of LTE UL degraded by a small fraction with a reduction of approximately 1 Mbps of data rate in the presence of TM system in the adjacent band. The LTE DL was fully functional, a clean constellation graph and maximum data rate were obtained.

LTE UL and TM both at 1780 MHz

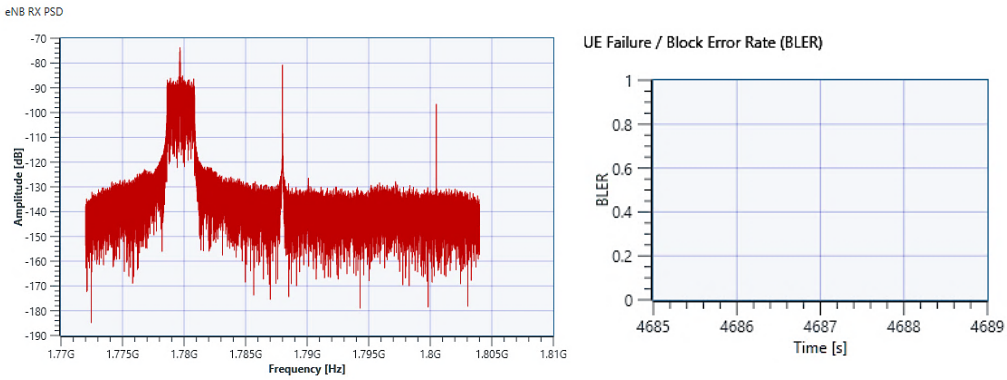

Figure 41: LTE UL and TM both at 1780 MHz with BLER.

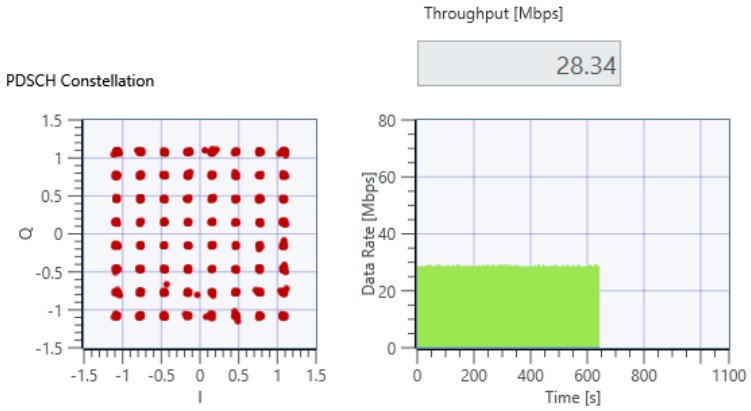

Figure 42: LTE UL constellation and data rate at 1780 MHz.

LTE DL and TM both at 2200 MHz

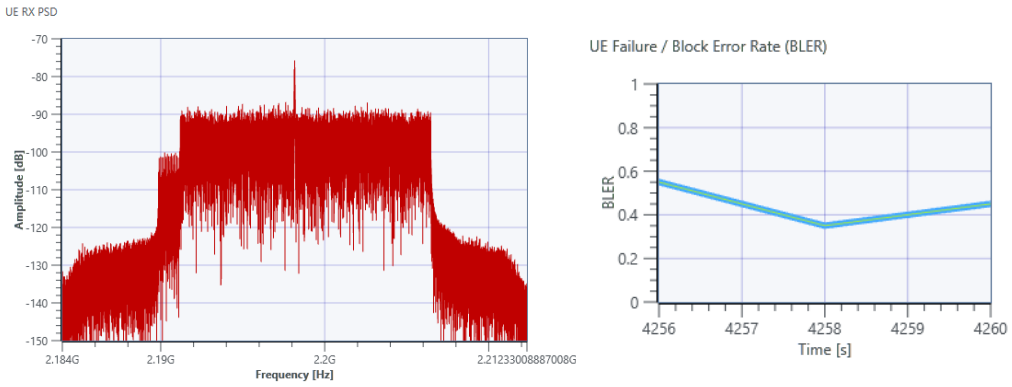

Figure 43: LTE DL and TM both at 2200 MHz with BLER.

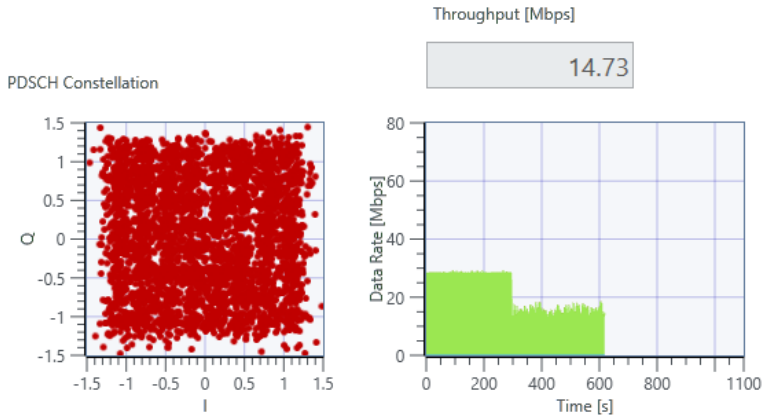

Figure 44: LTE DL constellation and data rate at 2200 MHz.

The in band LTE system performance were quite different from the adjacent band. The LTE UL was operational in the presence of TM system in the same band, but the LTE DL was hampered severely with high BLER, completely disrupted constellation graph and a significant drop in data rate which is approximately 50% lower than the baseline value.

5.4 BANDPASS FILTERING

The TM and LTE interference scenario was observed in the previous sections. A possible interference mitigation technique is using bandpass filter, which rejects the adjacent interfering signal. In this section we will analyze the performance of narrowband digital filters with different types of IIR filter and their order. Two signals centered at 500 kHz and 510 kHz are modulated using FDM. One of the adjacent signals which is centered at 510 kHz is filtered out using bandpass filtering techniques. The filtering techniques using several IIR filters: Butterworth, Chebyshev and Elliptic are among the popular ones. The power levels of the filtered-out signal will be measured, and the rejection criteria of the applied filter will be established.

5.4.1 Baseline With No Filtering

The Figure 45 shows the frequency domain representation of the AM signals without any application of bandpass filter. The LabVIEW Power Spectrum gives us the waveform of the signals in the frequency domain with their corresponding magnitudes.

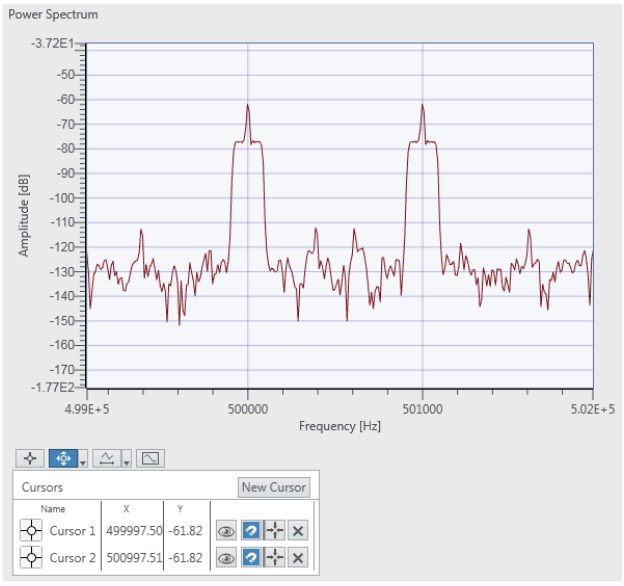

Figure 45: AM Signals with no filter.

Figure 46 shows the plot in MATLAB which were generated using the magnitude (dB) and frequency (Hz) values obtained from the LabVIEW power spectrum.

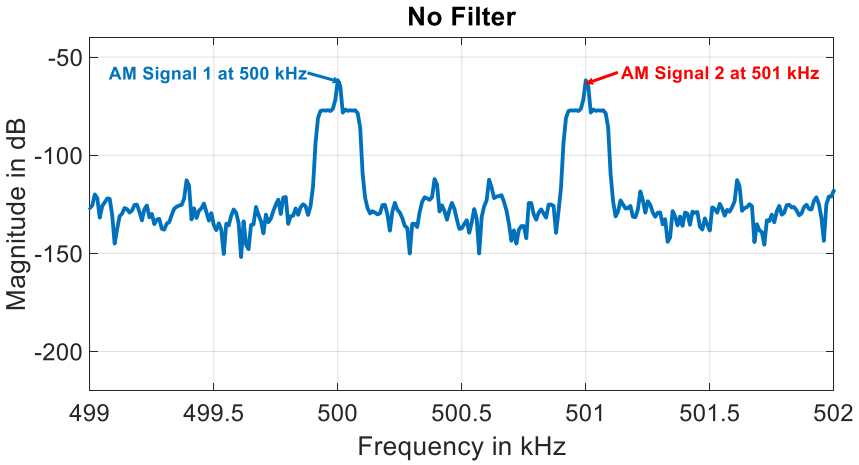

Figure 46: MATLAB plot of AM Signals with no filter.

5.4.2 Butterworth Filter

In this section we will demonstrate the performance of a Butterworth filter with orders 2, 5 and 10. The change in power levels of the adjacent signal after applying the filter will be measured and the filter profile will be demonstrated.

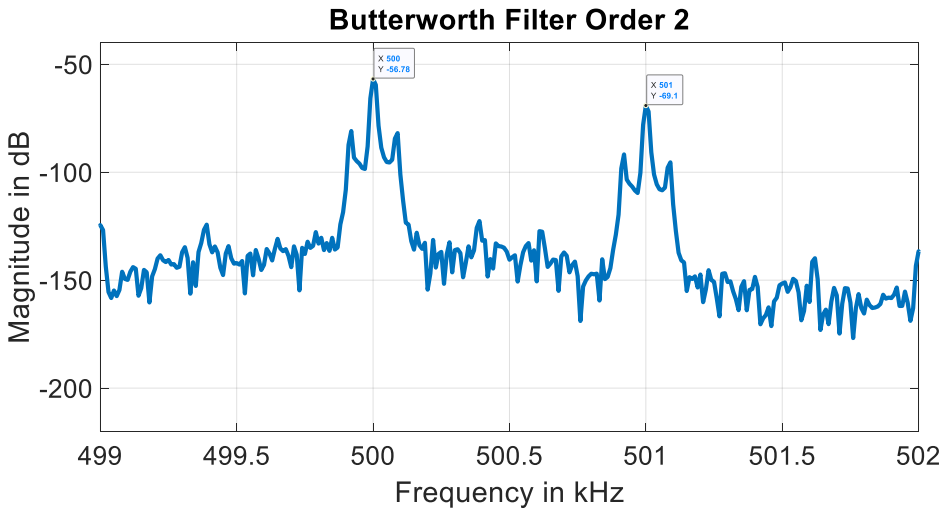

Figure 47: MATLAB plot of Butterworth filter with order 2.

The Figure 47 depicts the effect of an order 2 Butterworth bandpass filter on an adjacent interfering signal. The AM Signal 1 falls in the passband frequency of the bandpass filter centered at 500 kHz.

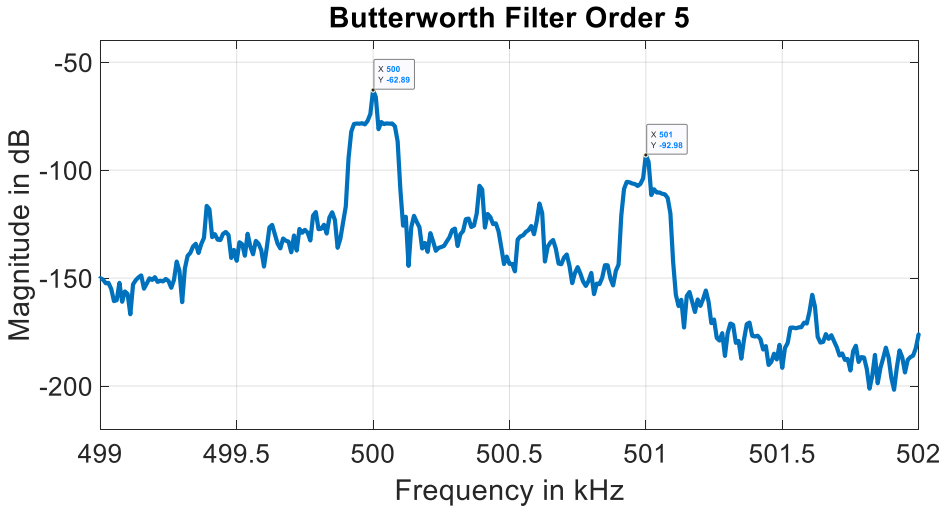

Figure 48: MATLAB plot of Butterworth filter order 5.

The rejection level increases with the increase in the Butterworth filter order.

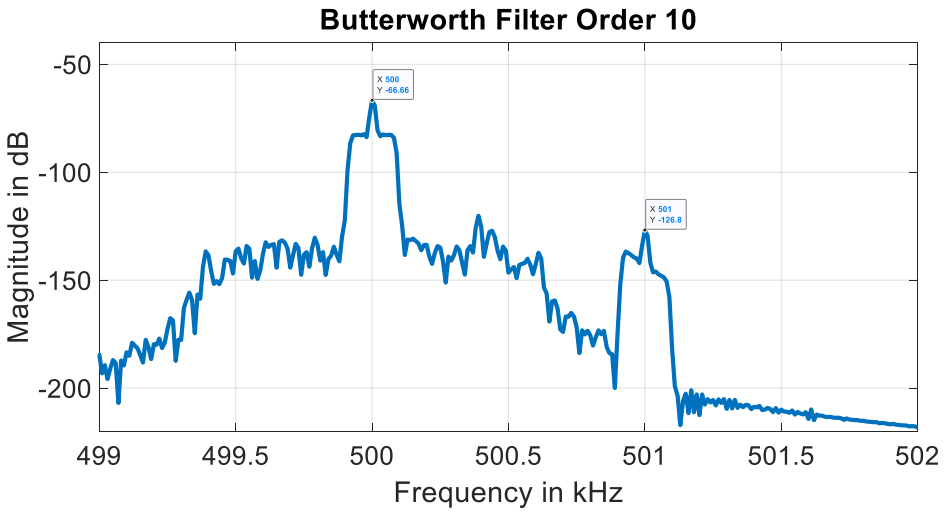

Figure 49: MATLAB plot of Butterworth filter order 10.

The last case of the Butterworth bandpass filter uses order of 10 which completely filters the interfering signal and reduces the power level of the interfering signal to a minimum, that is the noise floor.

Table 2: Summary of Butterworth filter performance

Filter Order#	**AM Signal 1 Power in dB**	**AM Signal 2 Power in dB**	**Rejection Level in dB**
2	-56.78	-69.1	12.32
5	-62.89	-92.98	30.09
10	-66.66	-126.8	60.14

5.1.2 Chebyshev Filter

In this section we will demonstrate the performance of a Chebyshev filter with orders 2, 5 and 10. The change in power levels of the adjacent signal after applying the filter will be measured and the filter profile will be demonstrated.

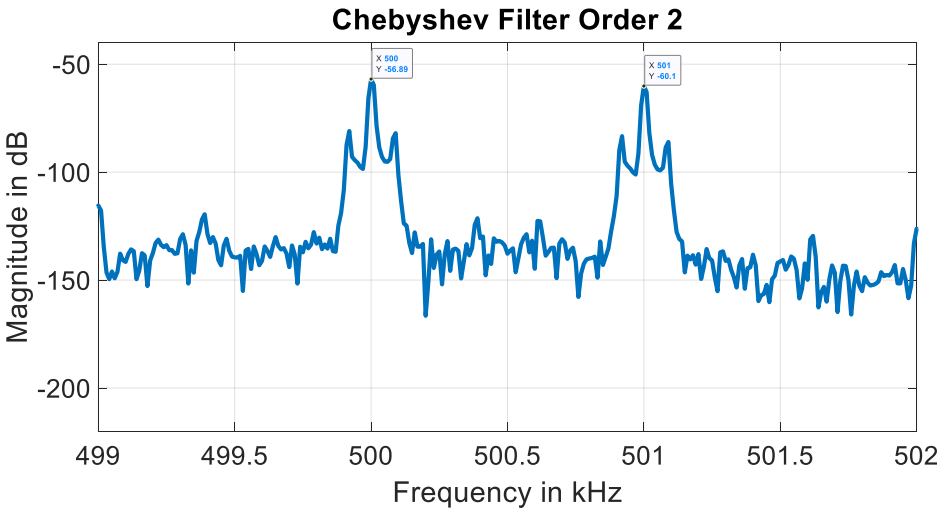

Figure 50: MATLAB plot of Chebyshev filter order 2.

The Chebyshev filter with order 2 has a rejection level which can be barely noticed. The rejection level is lowest among its competitors.

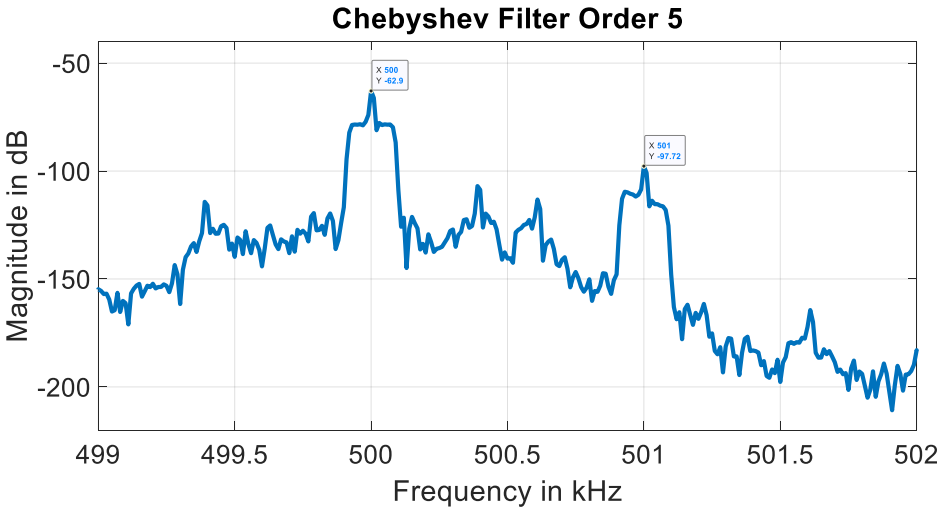

Figure 51: MATLAB plot of Chebyshev filter order 5.

There is a significant improvement in the rejection level of the Chebyshev filter with order 5, but it is still much lower than the Elliptic filter of the same order.

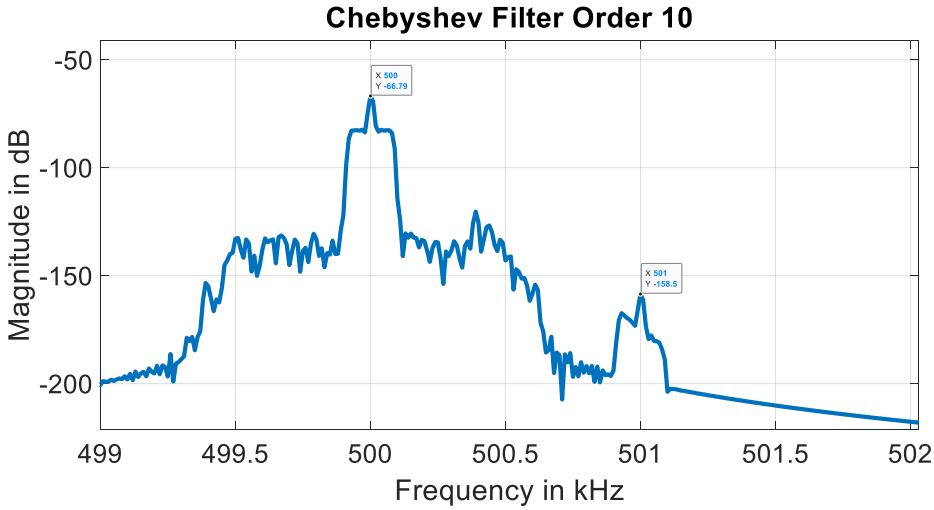

Figure 52: MATLAB plot of Chebyshev filter order 10.

Chebyshev filter with order 10 has an outstanding rejection level, highest among the other filter with the same order. The interfering signal is suppressed with minimal interference.

Table 3: Summary of Chebyshev filter performance

Filter Order#	**AM Signal 1 Power in dB**	**AM Signal 2 Power in dB**	**Rejection Level in dB**
2	-56.89	-60.1	3.21
5	-62.9	-97.72	34.82
10	-66.79	-158.5	91.71

5.4.3 Elliptic Filter

In this section Elliptic filters will be implemented with their performance being analyzed for comparison with the previous family of filters.

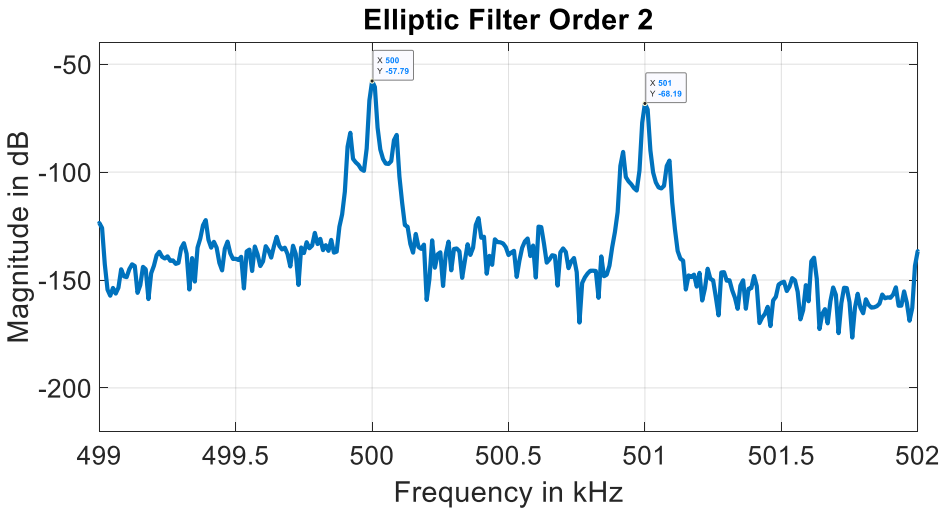

Figure 53: MATLAB plot of Elliptic filter order 2.

Elliptic filter with order 2 shows better rejection level than the Chebyshev filter but not as good as the Butterworth filter of the same order.

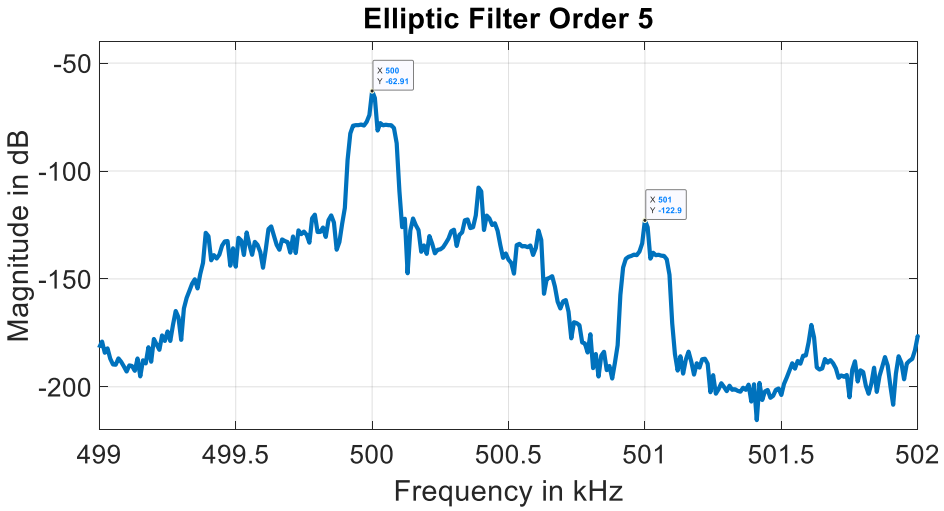

Figure 54: MATLAB plot of Elliptic order 5.

Elliptic filter with order 5 shows a drastic change in rejection level compared to the filter with order 2.

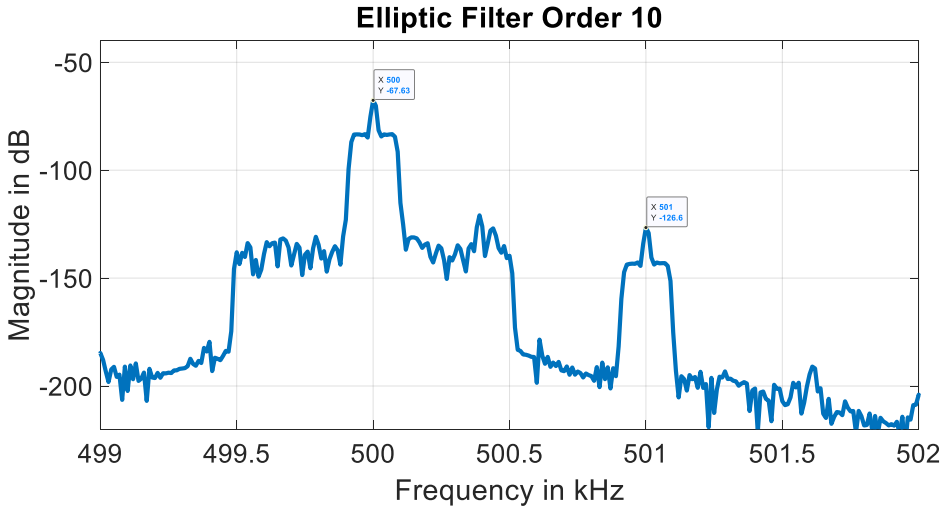

Figure 55: MATLAB plot of Elliptic filter order 10

The Elliptic filter with order 10 and 5 has similar performance with very close rejection levels.

Table 4: Summary of Elliptic filter performance

Filter Order#	AM Signal 1 Power in dB	AM Signal 2 Power in dB	Rejection Level in dB
2	-57.79	-68.19	10.4
5	-62.91	-122.9	59.99
10	-67.63	-126.6	58.97

5.4.4 Overview of Bandpass Rejection Levels

The overview of Butterworth, Chebyshev and Elliptic filter bandpass performance levels are demonstrated in Table 5.

Table 5: Overview of IIR filter performance

Filter Order#	Butterworth		Chebyshev		Elliptic	
	Signal Power (dB)	Rejection Level (dB)	Signal Power (dB)	Rejection Level (dB)	Signal Power (dB)	Rejection Level (dB)
2	-56.78	12.32	-56.89	3.21	-57.79	10.4
5	-62.89	30.09	-62.9	34.82	-62.91	59.99
10	-66.66	60.14	-66.79	91.71	-67.63	58.97

The Figure 56 demonstrates the performance graph of the family of Bandpass filters.

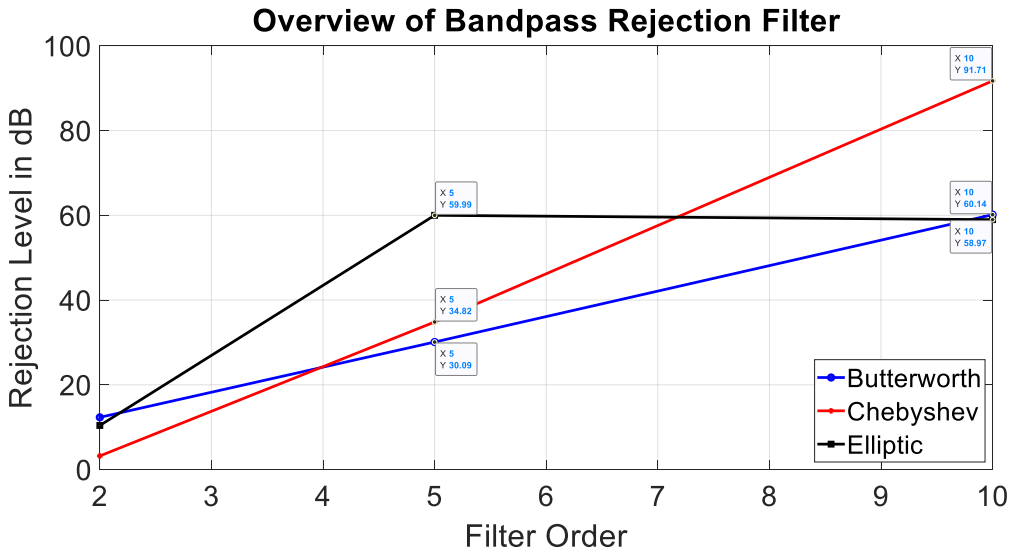

Figure 56: Overview of bandpass filter rejection levels.

5.5 Computational Methods in Signal Processing

The SDR testbed can be utilized to perform computational tasks using Mathscripts functionality in LabVIEW, instead of using the signal processing blocks. This section familiarizes

with a wireless communication scheme known as frequency division multiplexing and will use MATLAB code to receive sinusoid signals that have been modulated to different frequency bands. The issue of frequency offset in demodulation will also be examined.

Modulation, *demodulation*, and *filtering* are integral to the frequency division multiplexing (FDM) communication system. The purpose of this section is to familiarize with the implementation of these signal processing operations using simple sinusoidal signals.

5.5.1 Modulation

The purpose of this section is to understand the mechanics of modulation and demodulation as well as to study the effects of these operations on signals in the time and frequency domains using Mathscripts. To achieve this purpose, we will study the modulation and demodulation of a 1 Hz sinusoid by 10 Hz.

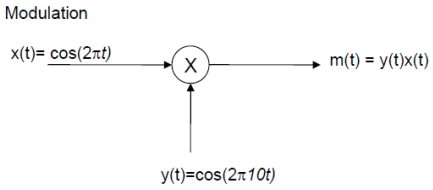

Figure 57: Modulation of information signal.

A sinusoid signal $x(t) = A\cos(2\pi f_1 t)$ is generated with frequency $f_1 = 1\,Hz$ and amplitude A of 1. The time domain representation of the signal is shown in Figure 58.

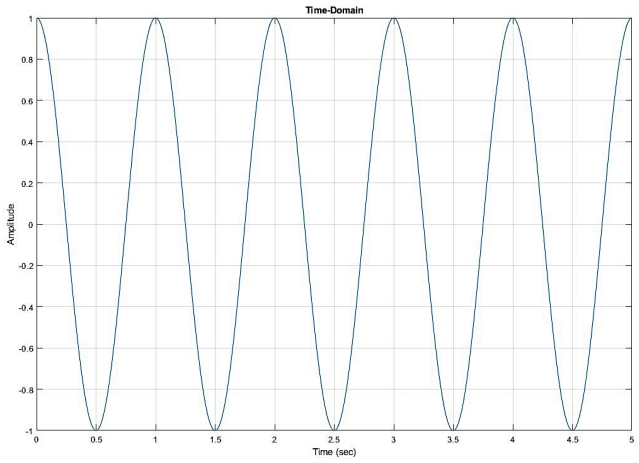

Figure 58: Time domain representation of information signal.

Now the magnitude of the spectrum of $x(t)$ is generated using the fft and $fftshift$ functions of MATLAB. Since $x(t)$ is a real signal, the magnitude of its spectrum is an even function (symmetric about 0 Hz). We expect to see a peak at 1 Hz and another at -1 Hz in the magnitude of the spectrum of $x(t)$.

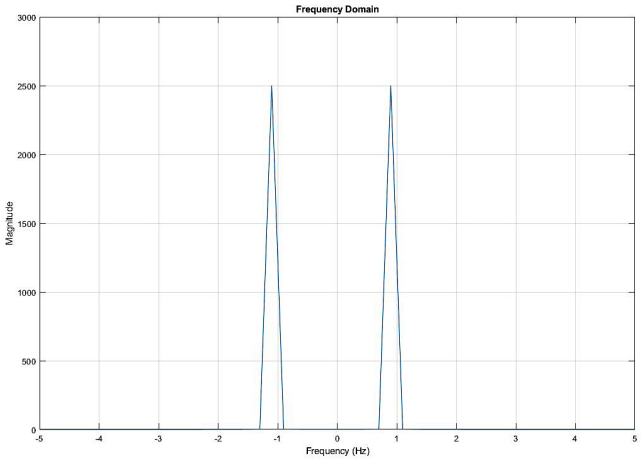

Figure 59: Magnitude spectrum of information signal.

The signal $x(t)$ is modulated upwards by 10 Hz. To do this we need to generate the modulating signal $y(t) = cos(2\pi f_2 t)$, and then create the modulated signal $m(t) = x(t)y(t)$. We can use simple trigonometric identity as well:

$$\cos(2\pi f_1 t) * \cos(2\pi f_2 t) = \frac{\cos\{2\pi(f_1 + f_2)t\} + \cos\{2\pi(f_1 - f_2)t\}}{2}$$

$$m(t) = \cos(2\pi t) * \cos(2\pi * 10 * t) = \frac{1}{2}\cos(2\pi * 11t) + \frac{1}{2}\cos(2\pi * 9t)$$

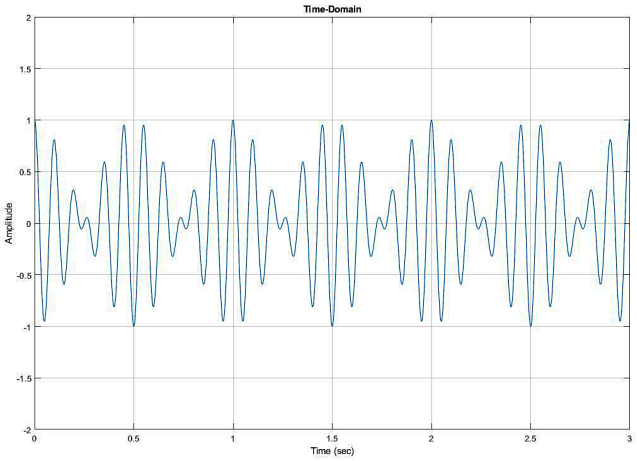

Figure 60: Time domain representation of modulated signal.

Now lets visualize the magnitude of the spectrum of $m(t)$. Since $m(t)$ is a real signal, the magnitude of its spectrum is an even function (symmetric about 0 Hz). A peak at +/- 9 Hz and +/- 11 Hz in the magnitude of the spectrum of $m(t)$ were seen as depicted in Figure 61.

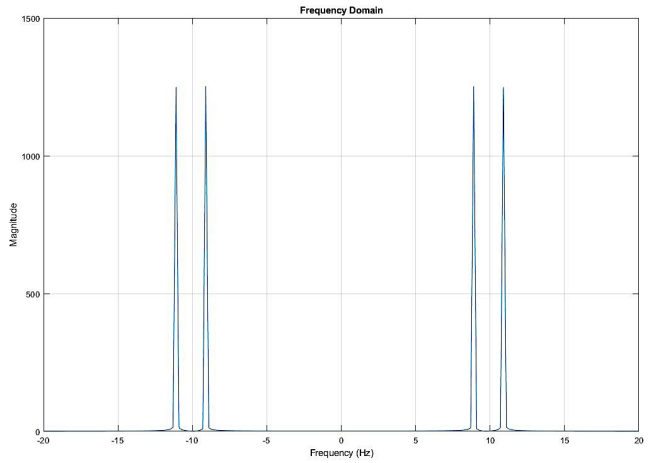

Figure 61: Magnitude spectrum of modulated signal.

5.5.2 Demodulation

Now the signal $m(t)$ is demodulated by 10 Hz in order to recover the signal $x(t)$. The modulated signal $m(t)$ is multiplied by $y(t)$ and the expression we get is $c(t)$,

$$ct(t) = \frac{1}{4}\cos(2\pi(f_1 - 2f_2)t) + \frac{1}{2}\cos(2\pi f_1 t) + \frac{1}{4}\cos(2\pi(f_1 + f_2)t)$$

$$c(t) = \frac{1}{4}\cos(2\pi * 19t) + \frac{1}{2}\cos(2\pi t) + \frac{1}{4}\cos(2\pi * 21t)$$

The time domain representation of $c(t)$ would be similar to $m(t)$.

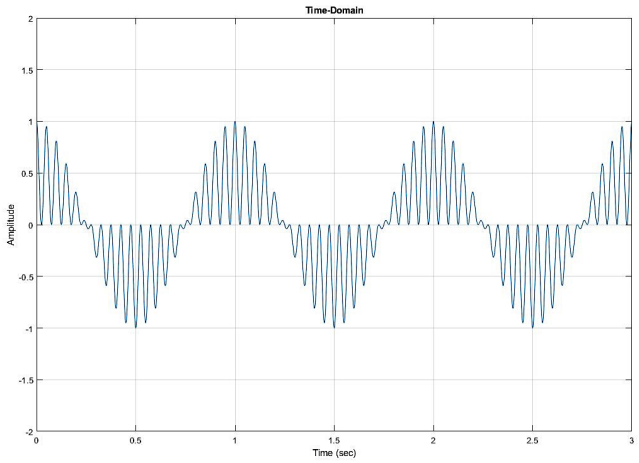

Figure 62: Time domain representation of demodulated signal.

Now visualize the magnitude of the spectrum of $c(t)$. Since $c(t)$ is a real signal, the magnitude of its spectrum is an even function (symmetric about 0 Hz). We expect to see a peak at +/- 21 Hz, +/- 19 Hz, and +/-1 Hz.

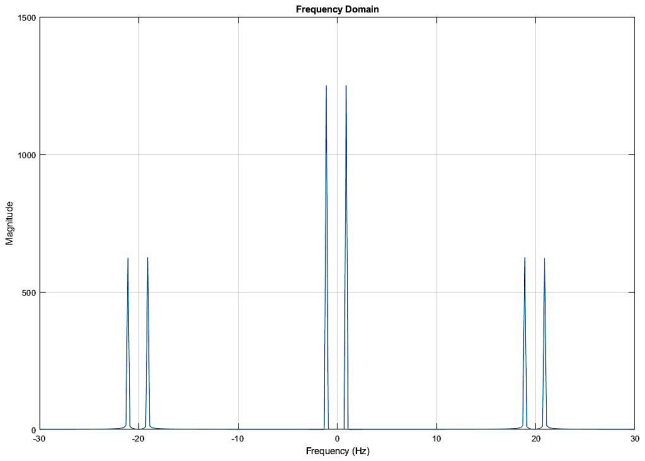

Figure 63: Magnitude spectrum of demodulated spectrum.

The higher frequency terms can be removed by applying lowpass filter to $c(t)$ to recover the original signal $x(t)$.

Chapter 6: Conclusion and Future Work

6.1 SUMMARY

The interaction between the adjacent radio frequency signals were observed on the SDR testbed. The interference on TM, and LTE system were evaluated in different RF bands. The adjacent band, out of band, and in band scenarios can be used to draw conclusion for possible mitigation techniques. Digital filtering techniques were also explored in the narrowband RF signals.

The TM system performance was evaluated in the presence of LTE system in three different cases: adjacent band, out of band, and in band. The TM system was fully functional in out of band experiments with the LTE system further apart. The TM system was functional with the LTE UL in the adjacent band, with the center frequencies 4 MHz apart from each other. The guard band between the two systems was approximately 1 MHz. Moreover, in the case of adjacent LTE DL system, the two systems were further apart from each other by 15 MHz with a higher guard band of approximately 5 MHz. The effect of LTE DL on TM system is much severe due to the aggressive modulation and higher signal power. The TM system performance was completely degraded by both the LTE UL and LTE DL system when they were overlapping with each other. Although both the systems operate in different bands but the in band experiments were done for a better understanding of the worst case scenario. The system performance for TM system included the FSER, constellation graph, eye diagram, and the power spectrum of the RX.

The LTE UL and DL system performance were also evaluated in the presence of TM system. The LTE system performance was satisfactory with the TM system in the adjacent band, and out of band. But even though LTE system uses more aggressive QAM modulation scheme,

whereas TM uses OQPSK modulation scheme, the LTE DL performance was hampered severely. This was observed in the in band experiments where TM system overlapped with LTE system. Again, this is not the usual case for the same reasons that the two systems operate in different bands. The LTE system performance parameters included: BLER, constellation graph and throughput or data rate measurements.

In order to explore interference mitigation technique and to utilize the full potential of the SDR testbed, further analysis was done using digital filtering approach. Digital filtering solution helps us to tackle interference from the system itself, as well as the adjacent RF signals. The performance of narrowband bandpass rejection filter was evaluated with different IIR filters: Butterworth, Chebyshev and Elliptic. The bandpass filtering capability in rejecting the adjacent interfering signal were demonstrated with different filter orders. The signal power and rejection level were measured, and comparisons made. The change in rejection level of the Butterworth and Chebyshev were linear corresponding to the change in filter orders. Whereas, the Elliptic filter rejection level dropped after reaching a peak value. The Butterworth rejection level is highest in the initial stages of filter order but as the order increased, Chebyshev rejection level wins the race and reaches a staggering value of 91.71 dB with an order of 10. The Chebyshev filter would be the best choice for our purpose since it delivers a rejection of 70 dB or more, compared to the analog filter acquired by WSMR.

The flexibility of the SDR testbed allowed us to evaluate system performance in different RF bands with the systems using different modulation scheme like TM and LTE. The interference levels were demonstrated with the numerical and visual parameters and possible mitigation techniques were laid out.

6.2 FUTURE WORK

In order to ensure the efficient use of the limited RF spectrum, a dynamic mitigation system will be developed, which will use computational methods on the SDR testbed to reduce the interference from the adjacent RF signals as depicted in Figure 10. The mitigation blocks M1, M2 and M3 will be equipped with mitigation solutions. Mitigation techniques will include digital filtering solutions, presented in Chapter 5: Results. Another technique will be to dynamically shift the frequencies to spectral bands, where there is reduced interference, also known as dynamic spectrum allocation.

The interference mitigation of existing TM and LTE system were tested and explained in this thesis paper. The data generated, for example the power spectral density, will be used for the classification of adjacent radio frequency users. Also, machine learning and neural network techniques will be implemented, to reduce the user intervention, and automatically detect the interference levels from the adjacent signals. This will be a computationally intensive task, and will explore the full potential of the SDRs. The next step would be to apply the mitigation techniques and analyze their performance in terms of the numerical and visual parameters, like the FSER, constellation graph, and the eye diagram demonstrated in this thesis paper. A SDR testbed with dynamic interference mitigation capabilities will be the end result, which is sometimes stated as Cognitive Radio Networks (CRN).

In future, the Internet of Things (IoT) and 5G devices will be adding more traffic in the bands of interest, adjacent to the TM system. The TM system will be given the highest priority in this case, making it the primary user for the dynamic mitigation system, in order to minimize interference from the adjacent users. The physical layout of the testbed presented in Figure 11, will remain same with more nodes to be added for testing purpose.

The most challenging task would be to implement the dynamic mitigation system using the SDRs in the licensed bands, that is allocated for mobile communication like the TM and LTE system. With the flexibility of the SDR testbed, all the systems will be operated with ease and without any violations to the FCC since it has the capability to work in a closed loop system. The TM system will be equipped with a mitigation system, that can either use digital filtering solution or the dynamic spectrum allocation, depending on the classification and detection of the interference levels from the adjacent signal.

6.3 TIMELINE

The study of dynamic interference mitigation of adjacent radio frequency signals on the SDR testbed will be performed according to the following timeline.

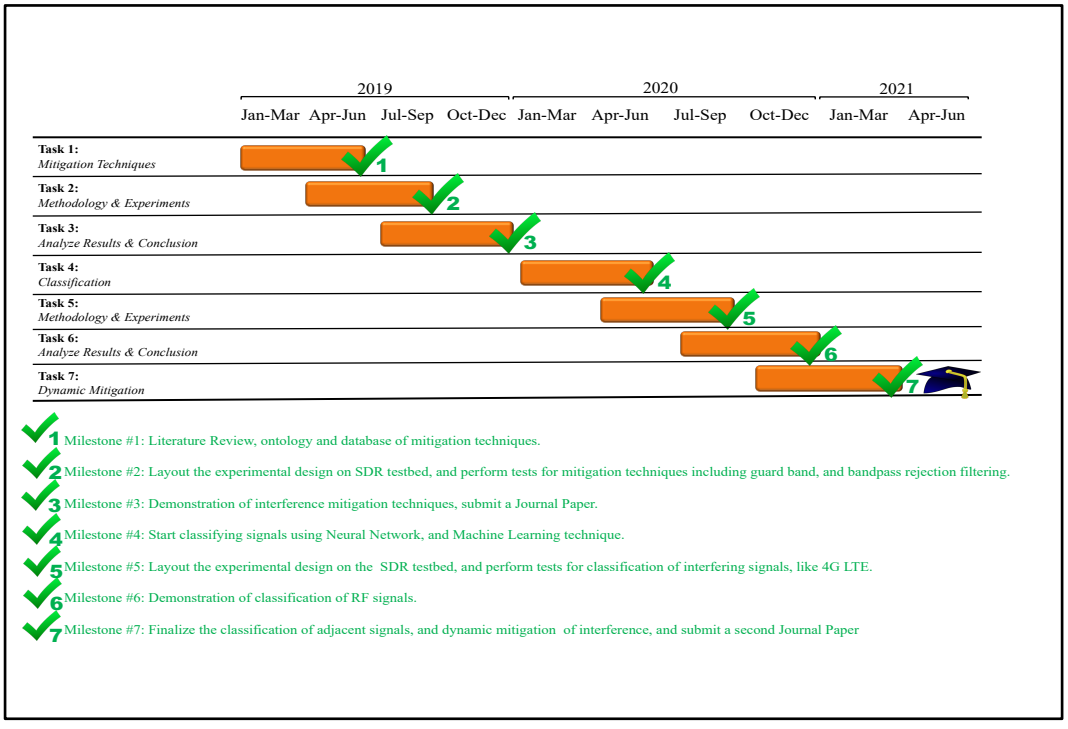

Figure 64: Timeline for the milestones to be completed for dynamic mitigation.

The tasks mentioned in the Figure 64, will be completed with the milestones being achieved. The Milestone 3 will conclude with the demonstration of mitigation techniques, and submitting a Journal Paper. The Milestone 7 will finalize the classification of adjacent signals, and dynamic mitigation of interference, and conclude by submitting a second Journal Paper for the Ph.D. Dissertation.

Literature review, ontology and database will be developed for the mitigation techniques and classification of signals mentioned in Task 1, and Task 4 respectively. Based on the study of mitigation techniques, and classification of adjacent interfering radio frequency signals, experiments will be performed on the SDR testbed and results will be demonstrated after Task 3 and Task 6. Finally, Task 7 would be to classify interfering signals, and perform dynamic mitigation, like using guard bands, or bandpass filtering, or frequency shifting.

References

[1] U. S. D. of C. Ntia, "Manual of Regulations and Procedures for Federal Radio Frequency - Table of Contents," *Channels*, no. May, 2009.

[2] "FCC Amendment of the Commission's Rules with Regard to Commercial Operations in the 1695- 1710 MHz, 1755-1780 MHz, and 2155-2180 MHz Bands," 2014.

[3] J. Proakis and D. Manolakis, *Digital Signal Processing*, Fourth Edi. 2007.

[4] "Intro Fundamentals of a RF Design ducti White Paper on to."

[5] "Commerce Spectrum Management Advisory Committee (CSMAC) Working Group 5 (WG 5) 1755-1850 MHz Airborne Operations," vol. 5, no. Wg 5, 1850.

[6] K. Temple, "an Initial Look At Adjacent Band Long-Term Evolution Wireless," no. July, 2016.

[7] B. Burn, S. Law, C. North, and R. Rigg, "Appendix A," vol. 11, no. June, pp. 1–8, 2017.

[8] J. F. Gonzalez, P. Rangel, V. Gonzalez, and D. Ph, "White Sands Missile Range (WSMR) Radio Spectrum Enterprise Testbed : A Spectrum Allocation Solution."

[9] J. F. Gonzalez, M. Elahi, J. A. Castillo, V. Gonzalez, P. Corral, and Y. Susumu, "4G Lte and Telemetry Interference Analysis on a Flexible Software-Defined Radio Testbed Platform."

[10] M. Elahi, J. Sandoval, and V. Gonzalez, "Performance Analysis of a Narrowband Bandpass Filter Rejection Level on a Flexible Software- Defined Radio Testbed Platform," *IEEE ICMIM*, 2019.

[11] M. Lofquist and N. Ctl, "Advanced Wireless Service 3 (AWS-3) Long- Term Evolution (LTE) Impacts on Aeronautical Mobile Telemetry (AMT) Test and Metrology Test Plan National Advanced Spectrum and Communications Test Network (NASCTN)," vol. 3.

[12] Z. Chen, N. Guo, and R. C. Qiu, "Building a cognitive radio network testbed," *Conf. Proc. - IEEE SOUTHEASTCON*, pp. 91–96, 2011.

[13] Z. Chen, Z. Hu, and R. C. Qiu, "Quickest spectrum detection using hidden Markov Model for cognitive radio," in *MILCOM 2009 - 2009 IEEE Military Communications Conference*, 2009, pp. 1–7.

[14] Z. Chen and R. C. Qiu, "Q-learning based bidding algorithm for spectrum auction in cognitive radio," in *2011 Proceedings of IEEE Southeastcon*, 2011, pp. 409–412.

[15] R. Zitouni, L. George, and Y. Abouda, "A Dynamic Spectrum Access on SDR for IEEE 802.15.4 networks," *arXiv Prepr. arXiv1505.02653*, 2015.

[16] "Radio Spectrum." [Online]. Available: https://en.wikipedia.org/wiki/Radio_spectrum.

[17] E. Series, "Software Defined Radio : 5 - 39 GHz."

[18] S. Smith, *The Scientist and Engineer's Guide to Digital Signal Processing*, Second Edi. California Technical Publishing, 1999.

[19] D. Filter, D. Toolkit, and U. Manual, "Digital Filter Design Toolkit User Manual," no. February, 2005.

[20] G. Ghosh, P. Das, and S. Chatterjee, "A Cognitive Radio And Dynamic Spectrum Access – A Study," *Int. J. Next-Generation Networks*, vol. 6, no. 1, pp. 43–60, 2014.

[21] A. Amraoui and B. Benmammar, "Dynamic spectrum access techniques state of the art," *Res. Methods Concepts, Methodol. Tools, Appl.*, pp. 139–157, 2015.

[22] L. Berlemann and S. Mangold, *Cognitive Radio and Dynamic Spectrum Access*. Wiley,

2009.
[23] B. A. Black, “Introduction to Communication Systems,” *LabVIEW Commun. with NI USRP*, 2014.

Glossary

3GPP	3rd Generation Partnership Project
4G	Fourth generation of Cellular technology
AM	Amplitude Modulation
AMT	Aeronautical Mobile Telemetry
AWGN	Additive White Gaussian Noise
BER	Bit Error Rate
BLER	Block Error Rate
BPF	Bandpass Filter
BW	Bandwidth
CR	Cognitive Radio
DL	LTE-Downlink Channel
eNB	eNodeB
FCC	Federal Communications Commission
FER	Frame Error Rate
FSER	Frame Synchronization Error
IQ	In-phase/Quadrature components

ISM	Industrial, Scientific, Medical radio frequency band
LTE	Long Term Evolution
NF	Noise Floor
NTIA	National Telecommunications and Information Administration
OFDM	Orthogonal Frequency-Division Multiplexing
OQPSK	Offset Quadrature Phase-Shift Keying
PDSCH	Physical Downlink Shared Channel
QAM	Quadrature Amplitude Modulation
RF	Radio Frequency
Rx	Receiver
SNR	Signal to Noise Ratio
TM	Telemetry
Tx	Transmitter
UE	User Equipment
UL	LTE-Uplink channel
WSMR	White Sands Missile Range

Appendix A

This section includes the information on amplitude modulated signals, and the characteristics of IIR bandpass filters that were observed in Chapter 5: Results.

A1.1 Software-Defined Radio

The NI USRP connects to a host PC creating a software defined radio depicted in **Error! Reference source not found.**[23]. Incoming signals at the SMA connector inputs are mixed down using a direct-conversion receiver to baseband I/Q components, which are sampled by an analog-to-digital converter (ADC). The digitized I/Q data follows parallel paths through a digital downconversion (DDC) process that mixes, filters, and decimates the input signal to a user-specified rate. The downconverted samples are passed to the host computer. For transmission, baseband I/Q signal samples are synthesized by the host computer and fed to the USRP at a specified sample rate over Ethernet, USB or PCI express. The USRP hardware interpolates the incoming signal to a higher sampling rate using a digital upconversion (DUC) process and then converts the signal to analog with a digital-to-analog converter (DAC). The resulting analog signal is then mixed up to the specified carrier frequency.

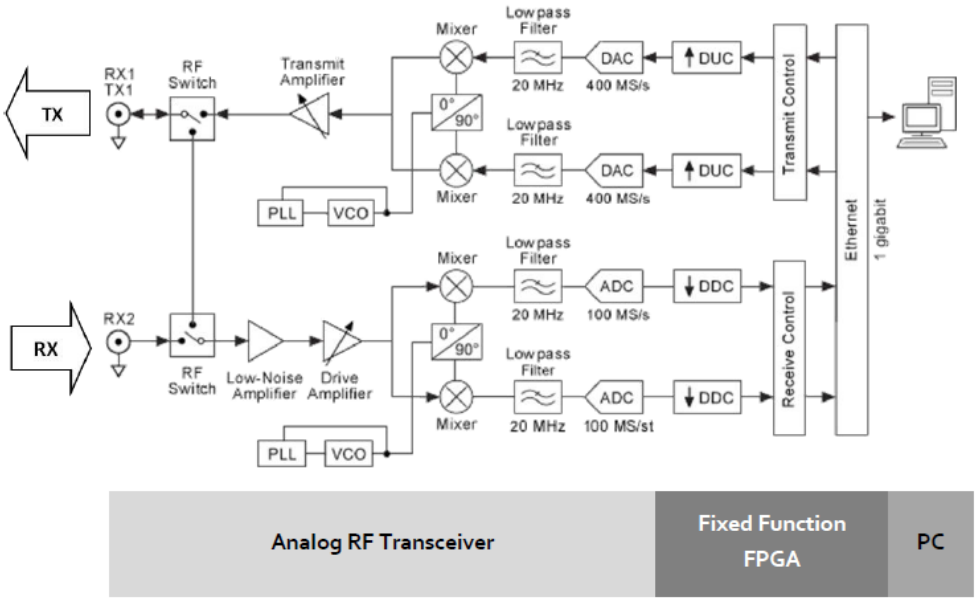

Figure 65: SDR architecture.

A1.2 Amplitude Modulation

This section lays out the process of generating Amplitude Modulation (AM) using SDR. It is considered to be the oldest of the modulation methods. A variety of systems use AM, including the AM broadcast radio.

If baseband message signal, m_t with a peak value of m_p and $A\cos(2\pi f_c t)$ is a carrier signal at carrier frequency f_c, then the AM signal $g(t)$ would be,

$$g(t) = A\left[1 + \mu\frac{m(t)}{m_p}\right]\cos(2\pi f_c t)$$

The parameter μ is the modulation index with values in the range $0 \leq \mu \leq 1$ in normal operation. Considering $m(t) = m_p\cos(2\pi f_m t)$ we can write,

$$g(t) = A[1 + \mu\cos(2\pi f_m t)]\cos(2\pi f_c t)$$

$$= A\cos(2\pi f_c t) + \frac{A}{2}\mu\cos[2\pi(f_c - f_m)t] + \frac{A}{2}\mu\cos[2\pi(f_c + f_m)t].$$

The above expression represents the carrier, lower sidebands and upper sidebands respectively. A plot is shown in **Error! Reference source not found.**.

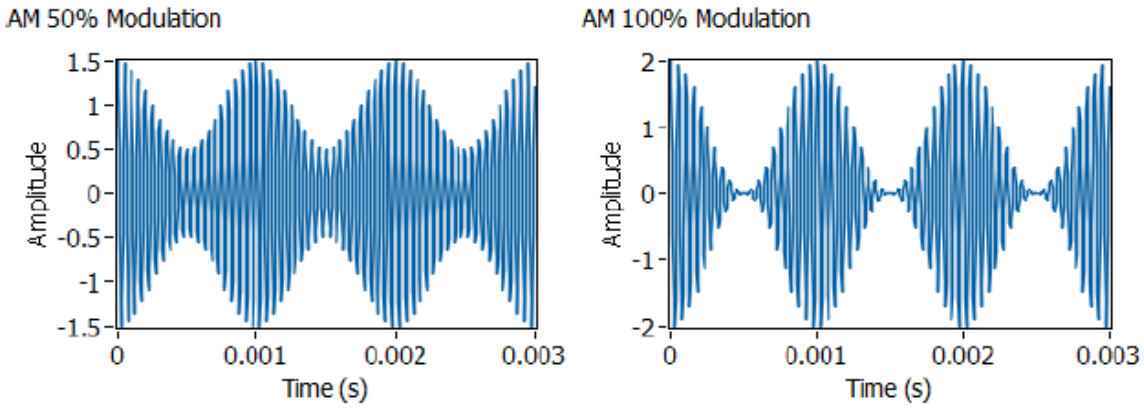

Figure 66: Amplitude Modulated Signals

When the AM signal arrives at the receiver, it has the form

$$r(t) = D\left[1 + \mu\frac{m(t)}{m_p}\right]\cos(2\pi f_c t + \theta),$$

where the carrier amplitude D is usually much smaller than the amplitude A of the transmitted carrier and the angle θ represents the difference in phase between the transmitter and receiver carrier oscillators. We will follow a common practice and offset the receiver's oscillator frequency f_o from the transmitter's carrier frequency f_c. This provides the signal,

$$r_1(t) = D\left[1 + \mu\frac{m(t)}{m_p}\right]\cos(2\pi f_{IF}t + \theta),$$

where the so-called "intermediate" frequency is given by $f_{IF} = f_c - f_0$. The signal $r_1(t)$ can be passed through a bandpass filter to remove interference from unwanted signals on frequencies near f_c. Usually the signal $r_1(t)$ is amplified as well.

Demodulation of the signal $r_1(t)$ is most effectively carried out by an envelope detector. An envelope detector can be implemented as a rectifier followed by a lowpass filter. The envelope A*(t)* or $r_1(t)$ is given by,

$$A(t) = D\left[1 + \mu\frac{m(t)}{m_p}\right] = D + D\mu\frac{m(t)}{m_p}$$

A1.3 Frequency Division Multiplexing

Frequency-division multiplexing is widely used in telemetry, in the satellite relaying of television signals, and, until the widespread adoption of fiber optics, was the standard transmission method for long-distance telephone signals. Frequency-division multiplexing also plays an important role in the OFDM technique used in DSL and in third-generation cellular telephone systems.

The two message signals $m_1(t)$ and $m_2(t)$ with subcarrier frequencies f_1 and f_2 are modulated,

$$g_1(t) = A_1\left[1 + \mu\frac{m_{1(t)}}{m_{1p}}\right]\cos(2\pi f_1 t\,)$$

$$g_2(t) = A_2\left[1 + \mu\frac{m_{2(t)}}{m_{2p}}\right]\cos(2\pi f_2 t\ )$$

If the subcarrier frequencies f_1 and f_2 are close to each other then will produce significant interference. Ideally, they should be spaced sufficiently apart in frequency so that the spectra of $g_1(t)$ and $g_2(t)$ do not overlap. The signals $g_1(t)$ and $g_2(t)$ are summed up to give,

$$g_I(t) = \ g_1(t) + g_2(t),$$

the in-phase component of the baseband signal. We will let the quadrature component $g_Q(t)$ equal zero for simplicity,

$$\tilde{g}(t) = g_I(t) + jg_Q(t) = g_I(t) = g_1(t) + g_2(t)$$

The actual signal transmitted would be,

$$g(t) = Ag_I(t)\cos(2\pi f_c t) - Ag_Q(t)\sin(2\pi f_c t) = A[g_1(t) + g_2(t)]\cos(2\pi f_c t)\,,$$

Where A is set by the gain parameter and f_c is the USRP carrier frequency.

Consequently, on the receiving side,

$$\tilde{r}(t) = D[g_1(t) + g_2(t)]e^{j\theta},$$

where θ is the phase difference between the TX and RX signal and $D << A$. This complex signal can be sent to a bank of two bandpass filters centers on the subcarrier frequencies f_1 and f_2. The filter outputs are the two different signals $g_1(1)$ and $g_2(t)$. These can be demodulated using the envelope detectors.

A1.4 Frequency Conversion

Generally, communication receivers convert a received signal at carrier frequency f_c to a signal at "intermediate" frequency f_{IF} for amplification and filtering prior to demodulation in the USRP. At the receiver we have the signal $r(t)$,

In the USRP, the frequency conversion can be carried out by offsetting the receiver's carrier frequency from the carrier frequency of the transmitted signal. To avoid confusion, the receiver's carrier oscillator is usually referred to as a "local" oscillator, and its frequency as the "local oscillator frequency" f_{LO}. We set the transmitter's carrier frequency to $f_c = 915.1\ MHZ$ and the receiver's local oscillator frequency to $f_{LO} = 915\ MHZ$. These settings provided an intermediate frequency $f_{IF} = f_c - f_{LO} = 100\ HZ$.

$$r(t) = A_r\left[1 + \mu\frac{m(t)}{m_p}\right]\cos(2\pi f_c t + \theta)$$

In the USRP receiver, frequency conversion is carried out in hardware by multiplying the received signal by $\cos(2\pi f_{LO}t)$ and by $-\sin(2\pi f_{LO}t)$. For example, suppose the received signal is the AM waveform

$$r(t) = A_r\left[1 + \mu\frac{m(t)}{m_p}\right]\cos(2\pi f_c t + \theta).$$

The receiver does the following,

$$r(t)\cos(2\pi f_{LO}t) = A_r\left[1 + \mu\frac{m(t)}{m_p}\right]\cos(2\pi f_c t + \theta)\cos(2\pi f_{LO}t)$$

$$= \frac{1}{2}A_r\left[1 + \mu\frac{m(t)}{m_p}\right]\cos(2\pi(f_c - f_{LO})t + \theta)$$

$$+\ \frac{1}{2}A_r\left[1 + \mu\frac{m(t)}{m_p}\right]\cos(2\pi(f_c + f_{LO})t + \theta)$$

The first term of the above equation is at the intermediate frequency $f_{IF} = f_c - f_{LO}$, while the second is at much higher frequency $f_c + f_{LO}$. The higher -frequency term is removed by filtering in the USRP, providing the "in-phase" component of the signal

$$r_I(t) = A_r \left[1 + \mu \frac{m(t)}{m_p}\right] \cos(2\pi f_{IF} t + \theta)$$

The receiver also forms a second signal,

$$\begin{aligned} -r(t) \sin(2\pi f_{LO} t) & \\ &= A_r \left[1 + \mu \frac{m(t)}{m_p}\right] \cos(2\pi f_c t + \theta) \sin(2\pi f_{LO} t) \\ &= \frac{1}{2} A_r \left[1 + \mu \frac{m(t)}{m_p}\right] \sin(2\pi (f_c - f_{LO}) t + \theta) \\ &= -\frac{1}{2} A_r \left[1 + \mu \frac{m(t)}{m_p}\right] \sin(2\pi (f_c + f_{LO}) t + \theta) \end{aligned}$$

The high frequency term is removed, and the receiver provides the quadrate signal

$$r_Q(t) = A_r \left[1 + \mu \frac{m(t)}{m_p}\right] \sin(2\pi f_{IF} t + \theta).$$

A conventional hardware-based receiver normally works with the in-phase signal given by $r_I(t)$. The USRP combines the in-phase and the quadrature signals to form the complex IF signal $\tilde{r}(t)$ given by

$$\begin{aligned} \tilde{r}(t) = r_I(t) + j r_Q(t) &= A_r \left[1 + \mu \frac{m(t)}{m_p}\right] \cos(2\pi f_{IF} t + \theta) \, \mathrm{j} \sin(2\pi f_{IF} t + \theta) \\ &= A_r \left[1 + \mu \frac{m(t)}{m_p}\right] e^{j(2\pi f_{IF} t + \theta)} \end{aligned}$$

This complex signal is what is actually provided to the user by Fetch RX Data module in the LabVIEW Communications Design Suite VI.

In the frequency domain, the spectrum $R(f)$ of the received signal $r(t)$ would be,

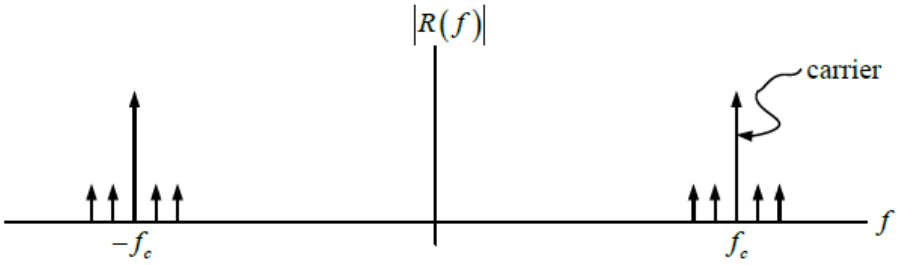

Figure 67: Frequency domain representation of the received signal.

Since $r(t)$ is a real-valued signal, its spectrum contains both positive and negative-frequency components. After frequency conversion, the complex IF signal $\tilde{r}(t)$ has the spectrum $\tilde{R}(f)$ containing only the positive frequency components,

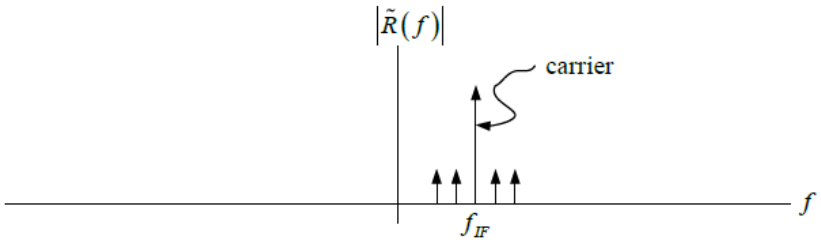

Figure 68: Rejecting the negative frequency component of the complex IF signal.

The complex IF signal goes through a bandpass filter with a frequency response in Figure 69. The goal is to reject signals other than the ones at carrier frequencies f_{IF}.

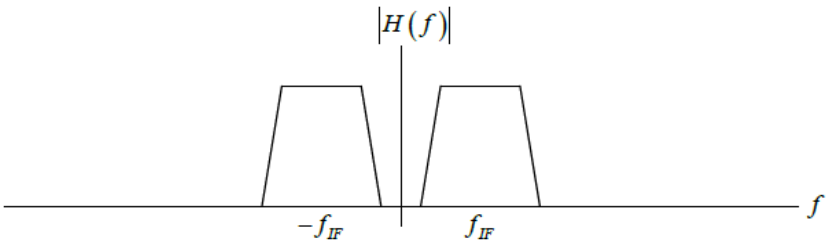

Figure 69: Frequency Response of Intermediate-Frequency Filter.

A1.5 Image Rejection

If a second signal is received along with the signal $r(t)$,

$$r_2(t) = A_{r2}\left[1 + \mu_2 \frac{m_2(t)}{m_{2p}}\right]\cos(2\pi f_{IM} t + \theta_2),$$

where carrier frequency f_{IM} is,

$$f_{IM} = f_{LO} - f_{IF}$$

After analyzing the above two equations, we get the complex IF of second signal $\tilde{r}_2(t)$ given by

$$\tilde{r}(t) = A_{r2}\left[1 + \mu_2 \frac{m_2(t)}{m_{2p}}\right] e^{j(-2\pi f_{IF} t + \theta_2)}$$

The signals $r(t)$ and $r_2(t)$ are said to be "images" of one another. A glance at the frequency response shown in Fig. X shows that both $r(t)$ and $r_2(t)$ will pass through the IF filter, and the two signals will interfere with each other in the demodulator that follows the IF filter. The relationship between the frequencies of the two image signals is worth noting. One signal, $r(t)$, is at a carrier frequency of $f_c = f_{LO} + f_{IF}$, while the other signal, $r_2(t)$, is at a carrier frequency of $f_{IM} = f_{LO} - f_{IF}$. These carrier frequencies are symmetrically arranged about the receiver's frequency f_{LO}, the way a physical object and its image are symmetrically distant from the surface

of a mirror.

A2.1 Bandpass Filtering

The bandpass filtering technique is applied on the narrowband AM signals to filter out the interference. Initially the specifications of the filter are designed. Then analysis of the characteristics of the resulting filter is performed to determine if the filter meets the requirements of the system. If the filter does not meet the requirements of the system, the specifications are modified, and the process is repeated. After an appropriate design of the filter is obtained, the filter is integrated in the system. To design a digital filter using LabVIEW, the filter type, sampling frequency, filter specifications, and design method must be specified.

The available filter types are lowpass, highpass, bandpass, and bandstop filters. A lowpass filter allows low frequencies to pass and attenuates high frequencies. A highpass filter allows high frequencies to pass and attenuates low frequencies. A bandpass filter allows a range of frequencies to pass and rejecting the stopband frequencies. A bandstop filter attenuates a range of frequencies and allows all frequencies not within the range to pass.

In Figure 70 symbol f_s denotes the sampling frequency, which is the expected rate at which the input signal for the filter is sampled. One-half of the sampling frequency is called the Nyquist frequency. X is the input signal to Filter. The $filter\ type$ specifies the passband of the filter with 0: Lowpass; 1: Highpass; 2: Bandpass; 3: Bandstop. The f_h is high cutoff frequency in Hz and f_l is the low cutoff frequency in Hz and both observe the Nyquist criterion. The $ripple$ is present in the passband and stopband which must be greater than zero and expressed in decibels. There is no ripple in Butterworth filter and only passband ripple in Chebyshev filter. The $order$ specifies filter order and is greater than 0. The $init/cont$ controls the initialization of the

internal states, the default is FALSE. To process a large data sequence that consists of smaller blocks, this can be set to FALSE for the first block and to TRUE for continuous filtering of all remaining blocks. The $Filtered\ X$ is the output array of filtered samples and the $error$ returns any error or warning from the VI.

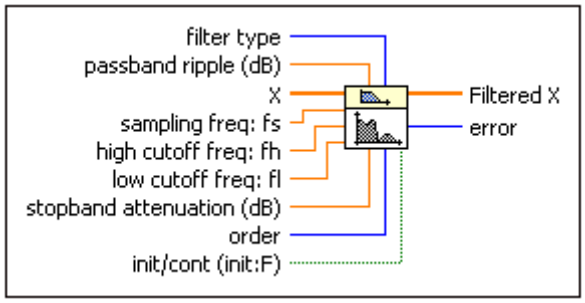

Figure 70: Filter parameters.

After invoking the Filter Coefficients VI, the Filter VI calls the IIR Cascade Filter VI to obtain a $Filtered\ X$ sequence. The values for f_h and f_s must observe the following relationship:

$$0 < f_1 < f_2 < 0.5f_s$$

where f_1 is low cutoff frequency f_l, f_2 is high cutoff frequency f_h, and fs is sampling frequency.

A2.2 IIR Filter Types

Digital IIR filter designs come from the classical analog designs and include the following filter types: Butterworth filters, Chebyshev filters, Chebyshev II filters, also known as inverse Chebyshev and Type II Chebyshev filters, Elliptic filters, and Bessel filters.

The IIR filter designs differ in the sharpness of the transition between the passband and the stopband and where they exhibit their various characteristics—in the passband or the stopband.

The following, Figure 71 illustrates the magnitude responses of a typical lowpass filter designed by the IIR filter design methods. Each filter has the same numerator and denominator order values.

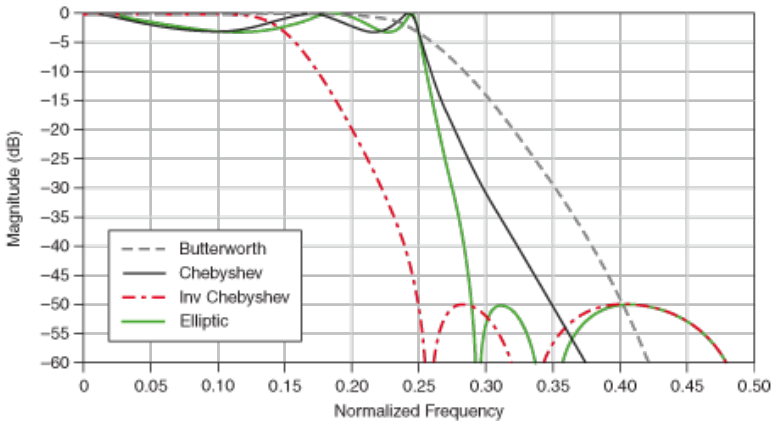

Figure 71: Typical filter response of Butterworth, Chebyshev, Inverse Chebyshev, and Elliptic filters.

The table below summarizes the main features of the IIR-based design methods so that the IIR filter design method can be determined.

Table 6: The IIR Filters and their characteristics.

IIR Filter	Ripple in Passband?	Ripple in Stopband?	Transition Bandwidth for a Fixed Order	Order fo Given Filter Specification
Butterworth	No	No	Widest	Highest
Chebyshev	Yes	No	Narrower	Lower

Elliptic	Yes	Yes	Narrowest	Lowest

A2.2.1 Butterworth Filter

The characteristics of Butterworth includes: smooth response at all frequencies, monotonic decrease from the specified cut-off frequencies, maximal flatness, with the ideal response of unity in the passband and zero in the stopband, and Half-power frequency, or 3 dB down frequency, that corresponds to the specified cut-off frequencies.

The advantage of Butterworth filters is their smooth, monotonically decreasing frequency response. Figure 72 shows the frequency response of a lowpass Butterworth filter.

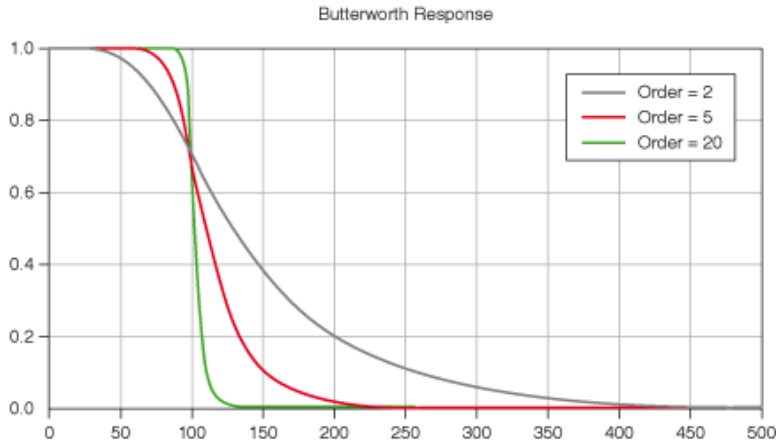

Figure 72: Typical Butterworth filter response with order 2, 3 and 20.

As shown in the previous figure, after the cut-off frequency of a Butterworth filter is specified, the steepness of the transition is proportional to the filter order. Higher order Butterworth filters approach the ideal lowpass filter response.

Butterworth filters do not always provide a good approximation of the ideal filter response because of the slow roll-off between the passband and the stopband.

A2.2.2 Chebyshev Filter

The characteristics of Chebyshev filters includes: minimization of peak error in the passband, equiripple magnitude response in the passband, monotonically decreasing magnitude response in the stopband, and sharper roll-off than Butterworth filters. Figure 73 shows the frequency response of a lowpass Chebyshev filter

Compared to a Butterworth filter, a Chebyshev filter can achieve a sharper transition between the passband and the stopband with a lower order filter. The sharp transition between the passband and the stopband of a Chebyshev filter produces smaller absolute errors and faster execution speeds than a Butterworth filter.

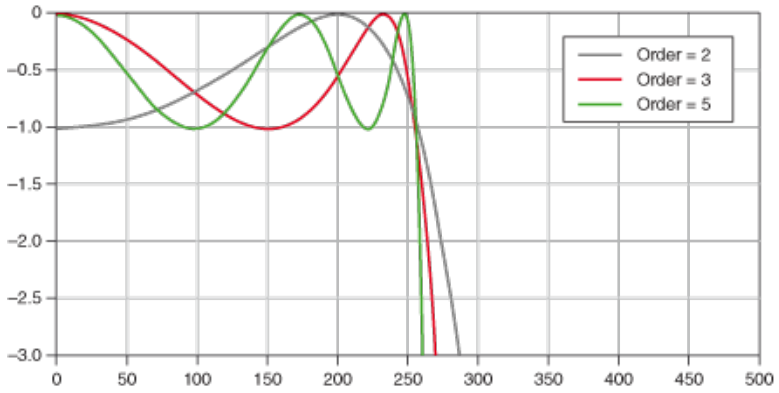

Figure 73: Typical Chebyshev filter response with order 2, 3 and 5.

In the previous figure, the maximum tolerable error constrains the equiripple response in the passband. Also, the sharp roll-off appears in the stopband.

A2.2.4 Elliptical Filter

Elliptic filters have the characteristics which includes: minimization of peak error in the passband and the stopband, and equiripples in the passband and the stopband. Figure 74 shows the frequency response of a lowpass elliptic filter.

Compared with the same order Butterworth or Chebyshev filters, the elliptic filters provide the sharpest transition between the passband and the stopband, which accounts for their widespread use.

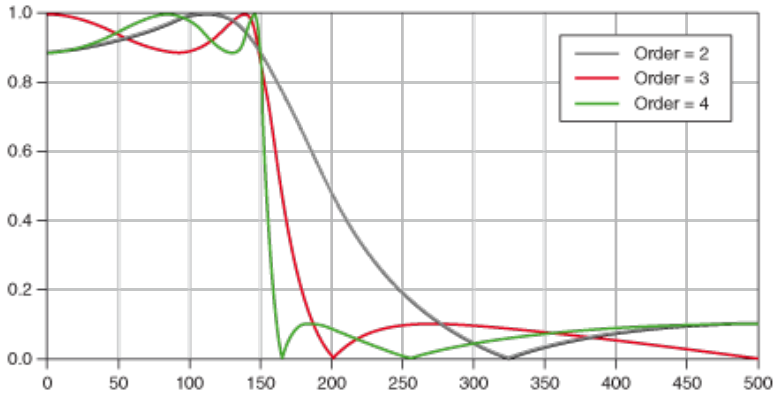

Figure 74: Typical Elliptic filter response with order 2, 3 and 4.

The same maximum tolerable error constrains the ripple in both the passband and the stopband. Also, even low-order elliptic filters have a sharp transition edge.

Appendix B

This section includes the MATLAB plots generated by the data obtained from the SDRs for the narrowband digital filtering experiments.

```
a = xlsread('all_data.xls'); %read .xls file

%% Plot of Adjacent Signals
t2   = a(:,20) * 1e-3;
m2   = a(:,21);

figure(1)
[pks,locs] = findpeaks(mc2,'MinPeakDistance',98); %mark the peaks
plot(t2, m2, t2(locs),pks,'or','Linewidth',5)     %plot with the peaks
grid on
ax = gca;
ax.FontSize = 32;
title('No Filter')
xlabel('Frequency in kHz')
ylabel('Magnitude in dB')
xlim([4.99e2 5.02e2])
ylim([-220 -40])

%% Plot Butterworth Filter Outputs

tb2   = a(:,1) * 1e-3;
mb2   = a(:,2);

tb5   = a(:,3) * 1e-3;
mb5   = a(:,4);

tb10   = a(:,5) * 1e-3;
mb10   = a(:,6);

figure(21)
plot(tb2,mb2,'Linewidth',5)
grid on
ax = gca;
ax.FontSize = 32;
title('Butterworth Filter Order 2')
xlabel('Frequency in kHz')
ylabel('Magnitude in dB')
xlim([4.99e2 5.02e2])
ylim([-220 -40])


figure(22)
plot(tb5,mb5,'Linewidth',5)
grid on
ax = gca;
ax.FontSize = 32;
```

```
title('Butterworth Filter Order 5')
xlabel('Frequency in kHz')
ylabel('Magnitude in dB')
xlim([4.99e2 5.02e2])
ylim([-220 -40])

figure(23)
plot(tb10,mb10,'Linewidth',5)
grid on
ax = gca;
ax.FontSize = 32;
title('Butterworth Filter Order 10')
xlabel('Frequency in kHz')
ylabel('Magnitude in dB')
xlim([4.99e2 5.02e2])
ylim([-220 -40])


%% Repeat for Chebyshev and Elliptic
%% Plot of Rejection Levels
x = [2 5 10];
y1 = [12.32 30.09 60.14];   %butterworth filter
y2 = [3.21 34.82 91.71];
y3 = [10.4 59.99 58.97];

figure(51)
plot(x,y1,'b-o',x,y2,'r-+',x,y3,'k-s','Linewidth',3)
ax = gca;
ax.FontSize = 32;
title('Overview of Bandpass Rejection Filter')
xlabel('Filter Order')
ylabel('Rejection Level in dB')
legend('Butterworth', 'Chebyshev', 'Elliptic','Location','southeast')
grid on
```

Vita

Mirza Mohammad Maqbule Elahi was born on November 15, 1991. The youngest child of Md. Fozle Elahi and Latifa Begum. Mirza graduated in Bachelor of Science (BS) in Electrical and Electronic Engineering (EEE) from Islamic University of Technology (IUT), Gazipur, Dhaka, Bangladesh in 2013. He worked as a Laboratory Instructor at North South University, Dhaka, Bangladesh for a period of two years before coming to University of Texas at El Paso (UTEP), El Paso, Texas to pursue Ph.D. in Computational Science from Fall 2016. He was appointed as a Teaching Assistant (TA) for Digital Systems Design I Laboratory, Mirza's duties included conducting the lab classes, preparing lab instructions for students, conducting experiments, monitor safety during the lab session, grading: quiz, assignment and other examinations, and proctoring during exam. He is currently a TA for the Microprocessors Systems class and the laboratory.

Mirza is working as a Research Assistant (RA) on Spectrum Management Project under the supervision of Dr. Virgilio Gonzalez beginning from September 2017. The project started as part of Army Research Lab (ARL) Academic Partnership with the regional Universities to mitigate the radio frequency interference encountered by Department of Defense (DoD) spectrum used by Telemetry (TM) at White Sands Missile Range (WSMR), New Mexico from major sources like 4G LTE mobile carriers using wireless prototyping techniques in a flexible Software-Define Radio (SDR) Testbed Platform. Mirza has expertise in using LabVIEW Communications Design Suite to prototype wireless systems.